Western&Graduate&PostdoctoralStudies

Electronic Thesis and Dissertation Repository

1-17-2018 1:00 PM

Pyrolysis as an Economical and Ecological Treatment Option for Solid Anaerobic Digestate and Municipal Sewage Sludge

Devon J. Barry, *The University of Western Ontario*

Supervisor: Briens, Cedric, *The University of Western Ontario*
Co-Supervisor: Berruti, Franco, *The University of Western Ontario*
A thesis submitted in partial fulfillment of the requirements for the Master of Engineering
Science degree in Chemical and Biochemical Engineering
© Devon J. Barry 2018

Follow this and additional works at: https://ir.lib.uwo.ca/etd

Part of the Chemical Engineering Commons

Recommended Citation

Abstract

The aim of this thesis was to investigate the potential for pyrolysis of solid anaerobic digestate and municipal sewage sludge. Slow, fast, and autothermal pyrolysis experiments were conducted for the anaerobic digestate while slow and fast pyrolysis experiments were carried out for the sewage sludge. Pyrolysis temperatures ranged from 250 to 550 ^{o}C. The effect of pyrolysis conditions on the pyrolysis products was examined.

For both anaerobic digestate and sewage sludge, fast pyrolysis at higher temperatures was favourable for energy recovery in the bio-oil products while, slow pyrolysis was favourable for the biochar products. Lower pyrolysis temperatures favoured energy recovery in the biochar, while higher temperatures increased biochar carbonization and stability. Soxhlet extraction of the biochar with deionized water showed that slow pyrolysis biochar performed better regarding the leachability of nutritive species and stability of heavy metals for the digestate and sewage sludge biochars respectively.

Autothermal pyrolysis increased the heating value of both the dry bio-oil and biochar products compared to traditional fast pyrolysis, but with a decrease in yield.

A new method for the calculation of the enthalpy of pyrolysis was developed and used to create a complete energy balance for the pyrolysis of sewage sludge. An economic analysis was completed for a sewage sludge pyrolysis plant. An environmental life cycle analysis was completed comparing the environmental effects of incineration and pyrolysis of sewage sludge. Pyrolysis of the sludge with the use of the biochar as a coal replacement was determined to have the greatest environmental benefit.

Keywords

Pyrolysis, Slow, Fast, Autothermal, Digestate, Sewage Sludge, Leaching, Enthalpy of Pyrolysis, Economic and Life Cycle Assessment

Acknowledgments

First, I would like to thank my supervisors; Dr. Cedric Briens, and Dr. Franco Berruti for their support, mentorship and guidance throughout my Masters. I would also like to thank Trojan Technologies and Mitacs Canada for providing funding and the opportunity to complete an internship during my study period. The value of the experience is immeasurable.

I would like to also extend thanks to my friends and colleagues from the Institute of Chemicals and Fuels from Alternative Resources (ICFAR). A special thanks goes out to Thomas Johnston, Venkat Reddy, Dr. Francisco J. Sanchez Careaga, Dr. Stefano Tacchino, and Dr. Dongbing Li for their technical support and training.

My appreciation also goes out to BioFuelNet Canada and the Ontario Clean Water Agency (OCWA) who provided project funding along with providing travel awards to attend conferences, meetings, and networking sessions.

Table of Contents

List of Tables

List of Figures

Chapter 1

1 Introduction and Background

1.1 What is Pyrolysis

Pyrolysis is the thermal cracking of organic matter in an inert atmosphere at elevated temperatures. The pyrolysis process is an endothermic reaction which transforms the solid organic matter into three products: a solid product called bio-char, a condensable vapour product called bio-oil, and a non-condensable gas product. The non-condensable gas stream, which consists mainly of CO, CO_2, CH_4, and H_2, (Shabangu et al., 2014) is usually combusted to provide heat for the pyrolysis reaction. The condensable vapours, also referred to as bio-oil, are usually the main product of biomass pyrolysis. Bio-oil is typically used as a fuel or upgraded and refined for specialty chemicals (Bridgwater, 2007). The solid product, biochar, consists mainly of carbon and the inorganics (ash) found in the biomass. Biochar has several potential uses including: use as a soil amendment, as a carbon neutral fuel, as an adsorbent, or other high value carbon applications such as a replacement for carbon black (Nanda et al., 2016).

The pyrolysis process conditions have a significant impact on the distribution and quality of the final products. By controlling certain process parameters such as reaction temperature, biomass heating rate, and vapour residence times it is possible to maximise the production of one product over the others and influence the product quality (Marshall, 2013). Three different pyrolysis regimes are classified as: slow pyrolysis, fast pyrolysis, and autothermal pyrolysis.

1.2 Slow Pyrolysis

Slow pyrolysis is defined by slow biomass heating rates (<10 °C/min) with long solid and vapour residence times. It is traditionally used for the production of charcoal as its primary product is biochar (Bridgwater et al., 2007). At higher temperatures the yield of biochar is found to slightly decrease while the permanent gas yield is found to slightly increase; the yield of liquid bio-oil peaks at an intermediate temperature. Reaction

temperature is the most significant parameter that affects product yields and quality in slow pyrolysis (Williams et al., 1996).

1.3 Fast Pyrolysis

Fast Pyrolysis is defined by high biomass heating rates (100-1000 ℃/min) and short vapour residence times (<2s) with rapid quenching of the pyrolysis vapours to prevent further cracking. This type of pyrolysis favours the production of liquid bio-oil (Bridgwater et al., 1999). The product distribution obtained during fast pyrolysis is a function of the cracking severity which can be described as a combination of the reaction temperature and the vapour residence time. Temperatures from 450-600 ℃ favour the production of bio-oil (Bridgwater et al., 2007). As the cracking severity increases, whether through increased reaction temperatures or vapour residence times, secondary cracking reactions occur increasing the yield of gaseous products while reducing liquid yields (Marshall, 2013). A typical product distribution for fast pyrolysis of woody biomass as a function of reaction temperature can be seen in Figure 1.1.

1.4 What is Biochar

For the extent of this thesis biochar refers to the solid product of biomass pyrolysis. Biochar consists mainly of carbon and of the minerals contained in the biomass (ash). Traditionally bio-oil has been viewed as the main product of pyrolysis but biochar has found many attractive applications due to its unique and adjustable physicochemical properties. The main reasons which cause biochar to be overlooked for use in high value applications are 1) the lack of standardized methods for characterisation, 2) the lack of standard biochar specifications for different applications, and 3) a knowledge gap regarding the impact of the biochar characteristics based on the pyrolysis feedstock and operating conditions (Lehmann et al., 2009).

These needs have begun to be addressed by the scientific community which has led to the development of organizations such as the International Biochar Initiative (IBI, 2017b) whose strategy is to promote collaboration on biochar research, provide dissemination of

knowledge, and create standards and policies to guide public in regulatory confidence.(IBI, 2017a). It has also steered the focus on biochar research away from viewing biochar as a "one size fits all" product towards "biochar by design"; where the production of biochar is tailored towards its end use application (Abiven et al.,, 2014).

Extensive work in the literature shows that pyrolysis temperature and heating rate are the main factors affecting the biochar properties (Bruun et al., 2017; Femi et al., 2012; Nanda et al., 2016; Shariff et al., 2016; Williams et al., 1996) . Figure 1.2 shows the relationship between pyrolysis temperature and biochar properties. In general as pyrolysis temperature increases, the biochar's alkalinity, aromatic carbon, ash content, specific surface area, and pore volume increase. However, biochar yield, electrical conductivity, cation exchange capacity, and volatile matter content decrease with an increase in pyrolysis temperature (Nanda et al., 2016).
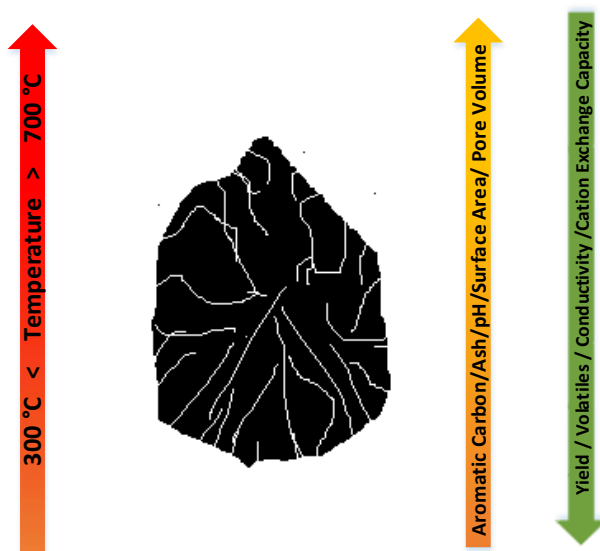
Figure 1.1: Effect of Pyrolysis Temperature on Biochar Properties, adapted from (Nanda et al., 2016)

These biochar properties are the main factors that determine the effectiveness of biochar in various applications. Some attractive biochar applications include: combustion as a source of renewable energy, soil amendment, carbon sequestration, activated carbons, and specialty materials (Abiven et al., 2014; Faria et al., 2017; Lehmann et al., 2009; Marchetti et al.,, 2013; Nanda et al., 2016; Yuan et al., 2013).

1.5 Sewage Sludge

Sewage sludge, also referred to as biosolids, is the by-product of municipal and industrial wastewater treatment plants. Sewage sludge is primarily water combined with the solids (both organic and inorganic) that are removed through physicochemical processes (settling, or filtration) during the wastewater treatment process. The global quantities of sewage sludge are expected to rise significantly over the next years due to increasingly strict effluent requirements for wastewater treatment plants, and the building of more wastewater treatment plants in developing countries (Agrafioti et al., 2013; Andreattola et al., 2006). With this increased sludge production, the necessity of an economic and environmentally sustainable treatment process is an important social issue (Hossain et al., 2011). The disposal or utilisation of sewage sludge is difficult to manage not only because of the large volumes produced, but also because of its high concentration of pathogens and heavy metals. Biosolids are primarily viewed as a waste stream. The main focus of biosolids treatment is to minimise its weight and volume to reduce disposal costs, while minimizing any potential health risks associated with its disposal. The traditional and most widely applied methods for the disposal of sewage sludge are: spreading on agricultural land, landfilling, and incineration with landfilling of ash (Agrafioti et al., 2013; Faria et al., 2017).

There has been ongoing debate over the use of sewage sludge on agricultural land in both Europe and North America. Due to the potential high level of heavy metals and pathogens contained within the sludge, there is concern about the impacts that use of the sludge on agricultural land has on human health and the environment.

Both the US EPA and the European Commission have developed specific requirements and guidelines concerning the use of sewage sludge on agricultural land. These guidelines include limits on heavy metals, pathogens, organic compounds, soil properties, and application rates (EPA, 1994; European Commission, 2001). Despite these guidelines several advanced nations do not support the application of biosolids to agricultural land. Netherlands and Belgium have prevented almost all use of sludge in agriculture since 1991. In Sweden, the Swedish Federation of Farmers recommends that their members stop using sludge on agricultural land. Farmers Unions in France, Austria, and Finland are also asking for a ban on the use of sewage sludge on agricultural land (European Commission, 2001).

Recently, there has been an interest in various thermal treatment techniques, including pyrolysis as an alternative method to utilise this waste stream.

1.6 Previous Studies on Sewage Sludge Pyrolysis

With respect to the production of biochar from the pyrolysis of sewage sludge, studies have shown that the temperature of pyrolysis is the most significant factor affecting biochar yield, as well as its physical and chemical characteristics. The biochar yield, as well as the percentage of energy recovered in the biochar product decreases with an increase in pyrolysis temperature (Hossain et al., 2011; Tan et al., 2014; Yuan et al., 2013).

Surface area of the biochar increases with an increase in temperature. Previous studies found that the surface area of sewage sludge biochar can be maximized at 90 m^2/g by impregnating the biochar with K_2CO_3 at 500 °C (Agrafioti et al., 2013). Without impregnation, the surface area of biochar from sewage sludge produced at this temperature is within the range of 18-25 m^2/g (Agrafioti et al., 2013; Tan et al., 2014; Yuan et al., 2013).

The enrichment of nutritive species in the biochar namely: nitrogen, potassium, and phosphorous show differing trends. Nitrogen is not found to be enriched in the biochar through pyrolysis, while phosphorous and potassium are both enriched in the biochar

through the pyrolysis process. The concentration of nitrogen remains relatively constant in the biochar with an increase in pyrolysis temperature, while both phosphorous and potassium concentrations are found to increase with an increase in pyrolysis temperature (Yuan et al., 2013). This is explained by nitrogen containing compounds being volatilized, along with other organic compounds, during the pyrolysis process while phosphorous and potassium remain in the solid state.

Biochar produced from sewage sludge shows potential benefits as a soil amendment. Soils amended with sewage sludge biochar have increased pH, total nitrogen, organic carbon and available nutrients (Khan et al., 2013). The most significant impact that sewage sludge biochar has on soil properties is the availability of phosphorous. Increases in nitrogen and sodium availability were also seen with sewage sludge biochar addition to soil. However, unlike other nutrients, an increase in the potassium availability in the soil was not seen (Faria et al., 2017; Khan et al., 2013; Sousa et al., 2015). Additional K supplementation would be required for soils amended with sewage sludge biochar. Biochar derived from sewage sludge has potential as a soil amendment, by increasing the availability of necessary plant nutrients.

Along with the availability of nutritive species, the stabilisation and availability of heavy metals from sewage sludge biochar is a concern due to their potential high concentrations in the biochar product. The concentration of heavy metals in the biochar increases through the pyrolysis process, as well as with an increase in pyrolysis temperature. However, the overall availability of the heavy metals has been found to decrease as a result of pyrolysis (Khan et al., 2013.; Méndez et al., 2012). The addition of sewage sludge biochar to soil decreased the bioavailable As, Cr, Co, Ni, and Pb, but increased the availability of Cd, Cu, and Zn. Although Cu and Zn are necessary micronutrients for plant growth, they can show toxic effects at higher concentrations. Some studies found that despite the increase in availability of Cd, Cu, and Zn, the concentrations of these metals within the crops grown on the amended soil did not exceed recommended limits (Khan et al., 2013). On the contrary (Faria et al., 2017) found that Cu concentrations in the plants grown in the sewage sludge biochar amended soil increased beyond recommended limits during the first year following biochar application. This confirms

that sewage sludge biochar with a higher concentration of Cd, Cu or Zn could pose a potential risk when added to agricultural soils. The bioavailability of metals in the soil could be linked to changes in soil cation exchange capacity, pH, and dissolved organic carbon values (Khan et al., 2013).

The addition of biochar produced from sewage sludge to agricultural soils shows an increase in plant productivity. Increases in plant yields have been seen for corn, radish, and rice grown in soils amended with sewage sludge biochar (Faria et al., 2017; Khan et al., 2013; Sousa et al., 2015). The increase in plant yields as a result of sewage sludge biochar addition were similar to the increase in yields achieved by the addition of NPK mineral fertiliser. It was found that the main factor affecting plant growth was the biochar's ability to provide macro and micro nutrients to the various plant species. In general the increase in soil fertility was proportionate to the increase of biochar applied (Sousa et al., 2015).

The addition of sewage sludge biochar can also reduce the emissions of greenhouse gas from the soil. (Sousa et al., 2015) Found that the application of sewage sludge biochar to soil decreased the emissions of CH_4 by more than 100%, which is to say that it became a CH_4 sink. N_2O emission reductions were also reported with cultivated soil having a reduction of 95.6-98.4 % (Sousa et al., 2015).

Overall, the addition of sewage sludge char has been found to benefit agricultural soils. The benefits are dependent on both the sewage sludge characteristics and site specific application details. However, there is a lack of studies that focus on optimizing the pyrolysis conditions for the creation of sewage sludge biochar to be used as a soil amendment.

Another application of interest for sewage sludge biochar is the use of the biochar as a solid fuel. The Sewerage Bureau of Tokyo Metropolitan Government has launched a project where dried sewage sludge is pyrolyzed to produce biochar which is sold as a coal substitute to thermal power generation plants (Oda, 2007). This plan was developed to promote the utilisation of sewage sludge and reduce greenhouse gas emissions. The main benefits of the process include:

- The biochar is considered a carbon neutral fuel which contributes to reduced CO_2 emissions from the power generation plant which uses the fuel.

- The biochar has a heating value of 8.4 MJ/kg which is approximately half that of coals. It can successfully be burned with coal at a power generation plant.

- Ease of handling of the solids is increased after pyrolysis, volume is reduced to $1/12^{th}$ of the initial volume and offensive odours are removed.

- Combustible gas generated by the sludge during pyrolysis is utilized as heat source for drying and carbonization which improves energy efficiency of the system.

A facility was built that can treat 300 tons of dewatered sludge per day. The cost to construct such a facility is around 5 Billion yen (56 Million $CAD), with operation and maintenance costs of around 5,000 yen (56 $CAD) per ton of dewatered sludge. These costs are comparable to the traditional procedure of incineration and dumping (Oda, 2007). The greenhouse gas reductions achieved through the facility are 37,000 tons of CO_2 equivalents.

Experiments to verify the operability and stability of the sewage sludge pyrolysis system were performed (Koga et al., 2007). In this system the pyrolysis gases and vapours are combusted to provide energy for the pyrolysis process. The system was found to be easily controlled and responsive to changes in the sewage sludge input. A thermal efficiency of 87.9% was achieved in a similar system without the need for additional energy inputs (Liu et al., 2017). An analysis of the products compared to the dewatered sewage sludge input can be seen in Table 1.1. Biochar produced from sewage sludge has been shown to be a viable fuel in thermal power generation plants. Energy efficiency of the pyrolysis process has been defined as a key parameter for the success of a sewage sludge pyrolysis plant.

Table 1.1: Sewage Sludge and Biochar properties adapted from (Koga et al., 2007)

	Dewatered Sludge	Pyrolysis Biochar
Water Content (wt% WB)	79.7	-
Ash Content (wt% -DB)	17.1	55.3
Combustibles Content (wt% -DB)	82.3	44.7
C (wt% -DB)	44.4	38.6
H (wt% -DB)	6.5	0.8
N (wt% -DB)	4.5	3
S (wt% -DB)	0.82	0.62
Cl (wt% -DB)	0.09	0.05
HHV (kJ/kg -DB)	20,040	13,950

1.7   Anaerobic Digestate

Anaerobic digestate (AD) is the effluent of an anaerobic digester after the biogas production process is complete. The composition of the digestate is determined by the digester feedstock and the digestion technology used (Wellinger et al., 2013). It is composed of solid and liquid fractions that together are called "whole digestate". The whole digestate is typically rich in nutrients with the solid fraction being high in carbon and phosphorous and the liquid fraction being rich in nitrogen and potassium (Fuchs et al., 2009). These two phases are usually separated. The benefits of this separating these fractions are end use dependent. Current interest is in the production of renewable fertilisers from digestate to replace mineral fertilisers.

Depending on the feedstock of the digester, various concentrations of heavy metals can be found in the solid fraction of the digestate. Because of this, limitations have been made on the maximum allowable concentration for use as a soil amendment. Figure 1.3

shows the maximum allowable heavy metal concentration for the solid digestate according to the Nutrient Management Act, Ontario Regulation 267/03 (Ontario, 2002)
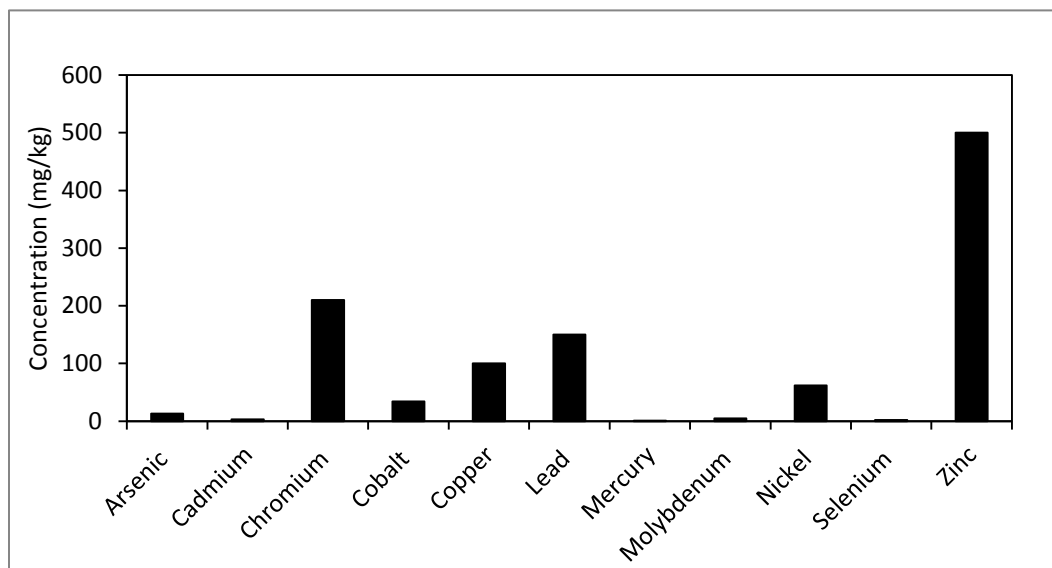
Figure 1.2: Maximum Allowed Metal Concentration in Digestate for Soil Amendment adapted from (Ontario, 2002)

1.8   Previous Studies with Pyrolysis and Digestate

The majority of literature on the pyrolysis of anaerobic digestate is focused on the production of biochar as an additive to improve the operation of anaerobic digesters, or as a soil amendment and fertilizer replacement.

The addition of biochar to anaerobic digesters has been shown to improve the digester performance. The addition of biochar was able to increase substrate utilisation, methane productivity, process stability and buffering capacity (Shen et al., 2017). Methane production was found to increase by over 25% and methane concentration in the biogas reached up to 95%. The biochar addition improved the anaerobic digestion process by providing surface area for the colonisation of microbes. Surface area of the biochar was found to be maximized at the pyrolysis temperature of 800 °C. At this temperature the BET surface area was measured to be >100 m^2/g, a significant increase from the digestate feedstock (<1 m^2/g) (Huang et al.,2017).

The addition of biochar to the digester also increases the fertilizer value of the digestate by increasing the concentration of the micro and macro nutrients: P, K, Ca, Mg, and Fe in the digestate solids (Shen et al., 2017, Fagbohungbe et al., 2016). Biochar can also be used to absorb nutrients such as phosphate from the liquid fraction of anaerobic digestate. (Kizito et al., 2017) found that the absorption of phosphate in the biochar was reversible and the regenerated biochar could reabsorb further quantities of phosphate. Biochar has potential for recovering and increasing the nutrient content of the liquid and solid digestate fractions respectively.

The availability and speciation of nutrients in biochar produced from anaerobic digestate has also been investigated. It is suggested that the main composition of the mineral ash in the char could exist as phosphates, carbonates, or oxides of alkali and alkaline earth metals (Huang et al., 2017). (Bruun et al., 2017) found that in the digestate solids the phosphorous was mainly in the form of simple calcium phosphates. It was also noted that large amounts of Mg could indicate the presence of struvite or other magnesium phosphates. At pyrolysis temperatures below 600 °C there was very little effect on P speciation but at higher temperatures more thermodynamically stable species, such as apatite, were formed. At severe pyrolysis conditions, temperatures exceeding 700 °C, volatilization of inorganic minerals were observed (Huang et al., 2017). Phosphorous availability in the soil was increased by the addition of pure digestate solids. However, despite the increase in phosphorous concentration in the biochars, only the biochar produced at 300 °C was able to increase phosphorous availability that exceeded or matched the phosphorous availability seen from the addition of the digestate solids. This is most likely explained by the formation of less soluble phosphorous species formed at the higher pyrolysis temperatures (Bruun et al., 2017). The availability of nutrients in biochar produced from anaerobic digestate can vary depending on the physicochemical properties of the char. Further investigation should look at optimizing the pyrolysis conditions for maximum release of nutritive species from the biochar.

The ability of digestate biochar to immobilise heavy metals in industrial soil is also considered as a potential application. Biochar created from anaerobic digestate was found to be more effective at immobilizing the heavy metals (Ci, Pb, Zn) in industrial soil than

biochars produced from more traditional sources including maize silage and wood pellets. Biochar produced at higher temperatures (600 °C) was found to perform better than biochar produced at lower temperatures (300 °C). It was found that the most important factors for decreasing the mobility of metals were having an alkaline pH, a high ash content to promote precipitation, increased functional groups, sufficient cation exchange capacity, and less labile carbon (Gusiatin et al., 2016) Biochar from anaerobic digestate is attractive as a large scale soil amendment for industrial soil.

Biochar from solid anaerobic digestate shows promise as an effective soil amendment. However there is a gap in the literature regarding the effect of pyrolysis conditions (temperature) and type (slow, fast, and autothermal) on its potential performance. At the time of writing no study comparing slow, fast, and autothermal of digestate could be found.

1.9 **Research Objectives**

The main aim of this thesis was to investigate the potential for pyrolysis of solid anaerobic digestate and municipal sewage sludge. The desired outcomes from each feedstock were dependent on the end use, the characteristics of the feedstock, and the needs of the project partners.

Anaerobic Digestate

- The main objective was to optimise the pyrolysis conditions to produce a biochar with high leachability of the plant macronutrients of P, K, Ca, and Mg for use as a soil amendment.

- Additional benefits to be considered were thermal self-sufficiency in the pyrolysis process and excess energy production through utilisation of pyrolysis co-products.

Sewage Sludge

- The main objective for the pyrolysis of sewage sludge was to optimise the pyrolysis conditions to create a thermally self-sustainable process, while meeting or exceeding the limitations of heavy metals for agricultural use, and minimizing their leachability.

- Additional benefits to be considered were the potential for biochar use as a solid fuel, as well as the economic and environmental impacts of implementing the sewage sludge pyrolysis process.

Chapter 2

2   Materials and Methods

2.1   Feedstocks

2.1.1   Anaerobic Digestate

The anaerobic digestate used in this study was delivered by Bayview Flowers Ltd located in Lincoln, Ontario, Canada. The digester input is a mixture of greenhouse and agricultural wastes, dairy manure and restaurant waste. This digestate, a slurry of liquid and solids, is partially separated using a screw press to reduce the moisture content to approximately 66 wt%. Table 2.1 shows an analysis of the digestate feedstock performed by E3 Laboratories.

Upon delivery, the digestate solids had a moisture content of 75 wt% and were dried in a greenhouse until a moisture content of less than 20 wt% was achieved. The solids were then stored indoors in a super sack until used for experimentation. For continuous processing the solids were milled to a particle size of 1 mm using a hammer mill. For batch processing the solids were not milled.

Table 2.1: Digestate Analysis (as delivered, analyzed by E3 Laboratories)

Regulated metals (maximum concentration allowed (mg/kg)	Result (mg/kg)
Arsenic (13)	<1.00
Cadmium (3)	<0.50
Chromium (210)	2.08
Cobalt (34)	<0.30
Copper (100)	13.1
Lead (150)	<0.40
Mercury (0.8)	<0.15
Molybdenum (5)	<0.30
Nickel (62)	<1.00
Selenium (2)	<1.00
Zinc (500)	20.8

2.1.2   Sewage Sludge

The sewage sludge used in this study was sourced from the Greenway wastewater treatment plant in London, Ontario. The Greenway wastewater treatment plant utilizes what is called activated sludge sewage treatment shown in Figure 2.1. After initial screening and grit removal the wastewater flows to a primary settling tank to remove the large organic solids. These solids settle out by gravity and are pumped to a sludge storage tank. After the primary settling tank the effluent is sent to aeration tanks to stabilise dissolved and fine, suspended impurities. After the aeration process the effluent goes into a final settling tank where the solids settle out by gravity as activated sludge. A portion of this activated sludge is fed back to the aeration section to maintain bacteria counts and the remainder is mixed with the primary sludge in a sludge storage tank (City of London, 2017).

Excess sludge from each wastewater treatment plant in London is trucked to Greenway and mixed with the Greenway sludge in the storage tanks. This mixed sludge is then pumped to centrifuges where it is mixed with polymer and dewatered to 72 wt% moisture. It is this dewatered sludge that was used for pyrolysis experiments.

After retrieving the sludge samples from the Greenway wastewater treatment plant the sludge was dried in an oven at 105 °C. For both batch and continuous pyrolysis experiments, the dried sludge was milled to a particle size of 1 mm using a hammer mill.
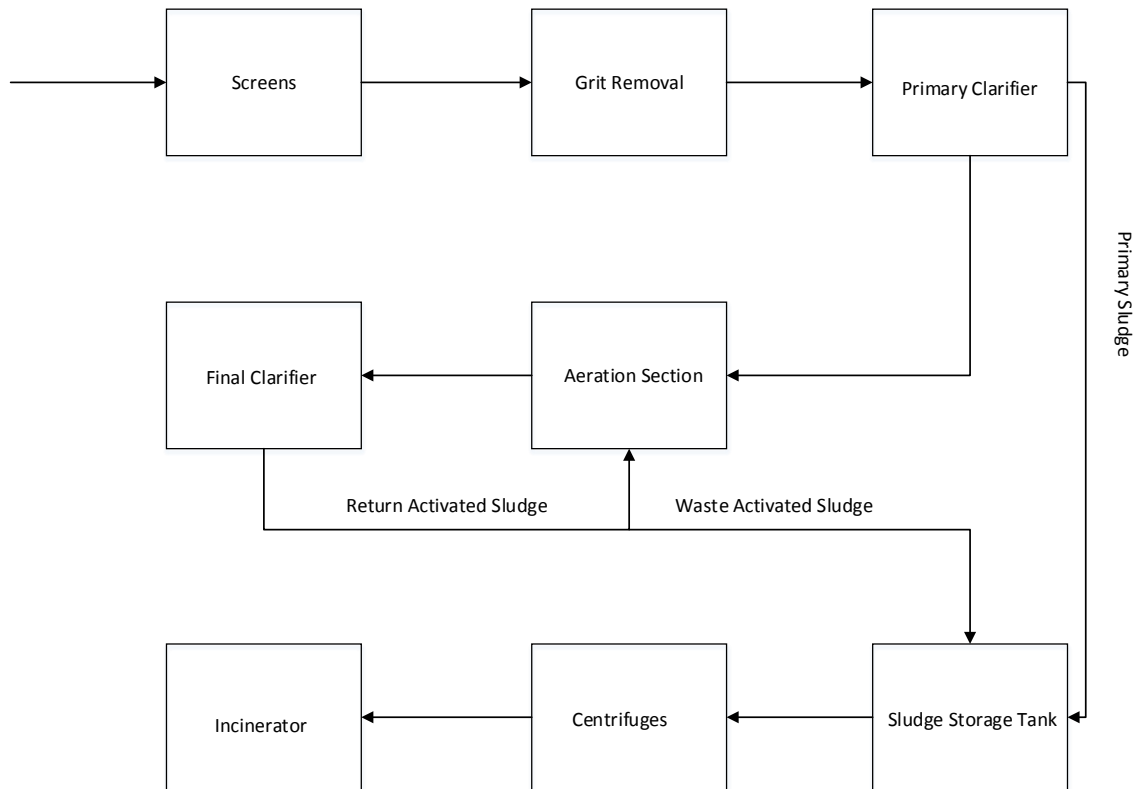
Figure 2.1: Greenway's Activated Sludge Process

Restricted Metal	Greenway Dewatered Sludge	Class A Maximum	Exceptional Quality Limit
As	<1.25	75	41
Cd	0.49	85	39
Cr	2	3000	12000
Cu	350	4300	1500
Mo	2	75	0
Ni	10	420	420
Pb	45	840	300
Se	<1.25	100	36
Zn	443	7500	2800

Table 2.2: Restricted heavy metal analysis of dewatered sewage sludge (all values in mg/kg)(EPA, 1994)

Table 2.2 shows the concentration of heavy metals in the collected sewage sludge from the Greenway WWTP as well as the maximum limits acceptable for land application as defined by (EPA, 1994). The collected sludge meets Class A limits for biosolids, which mean it is possible to apply these solids to agricultural land after the necessary pathogen and vector attraction reductions achievable through pyrolysis (EPA, 1994).

2.2   Slow Pyrolysis

2.2.1   Slow Pyrolysis Equipment
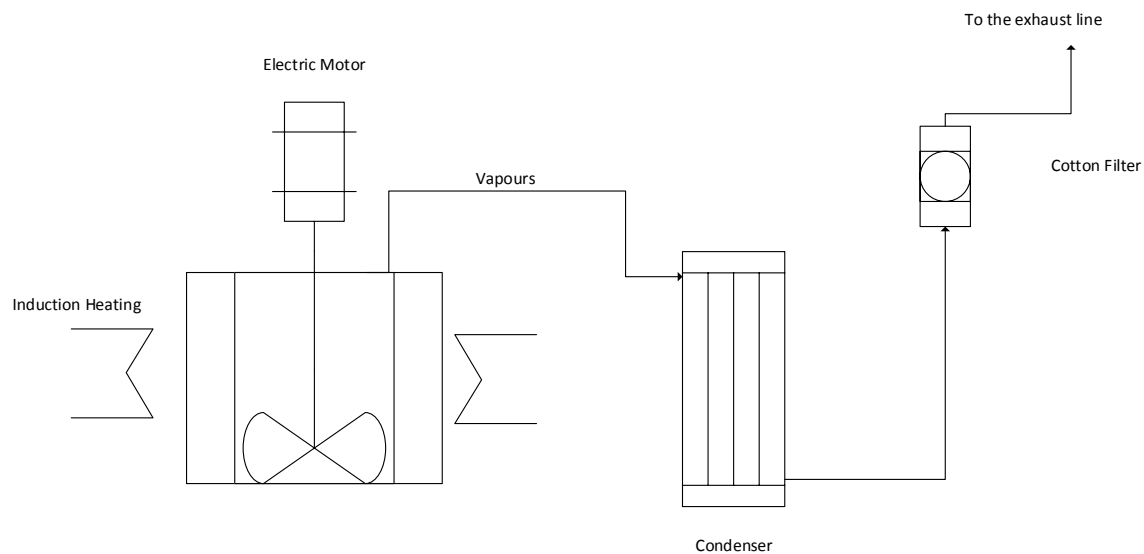
Figure 2.2: Batch MFR Diagram

The experiments for slow pyrolysis were performed in a batch Mechanically Fluidised Reactor (MFR) as shown in Figure 2.2. The reactor was cylindrical and constructed of 316 stainless steel. The dimensions of the reactor are shown in Table 2.3.

Table 2.3: MFR Dimensions

Dimension	Value
Wall Thickness	3.2 mm
Internal Diameter	10.15 cm
Internal Height	12.7 cm
Internal Volume	1.03 L

The mechanically fluidized reactor used an internal vertical blade stirrer, shown in Figure 2.3, to achieve the mixing performance of a traditional fluidized bed without requiring any fluidization gas (Lago et al., 2015). The stirrer also periodically (every 3 seconds) changed its direction of rotation to increase the heat transfer between the reactor wall and bed materials (Kankariya et al. 2016).

Figure 2.3: Vertical Blade Stirrer

The reactor bed temperature was controlled by an 1800 W induction heating system with an on-off controller. A software created using the LabWindows™/CVI platform (National Instruments, Austin, TX) recorded temperatures from the reactor bed, wall, freeboard, and condenser exit using K-type thermocouples.

The condenser consisted of a stainless steel tube condenser kept in a bubbling ice bath to collect condensable vapours. After the condenser the gases passed through a cotton demister to collect any aerosols that were not collected in the tube condenser. The gases were then vented.

2.2.2 Slow Pyrolysis Experimental Methods

To perform a batch slow pyrolysis experiment, 60-100 grams of biomass were added to the reactor at room temperature. The stirrer speed was set to 30 rpm for all experiments. The reactor was then heated from room temperature to the desired final pyrolysis temperature at a heating rate of 10 °C/min. Once the final reaction temperature was reached, it was maintained for 30 minutes before cooling the reactor back down to room temperature. The residence time of the vapours was not controlled or measured.

The char yield was determined by weighing the reactor before and after each experiment. The bio-oil yield was determined by weighing the condenser and cotton filter before and after each experiment. The non-condensable gas yield was determined by difference.

2.3 Fast Pyrolysis Equipment

2.3.1 Fast Pyrolysis Equipment
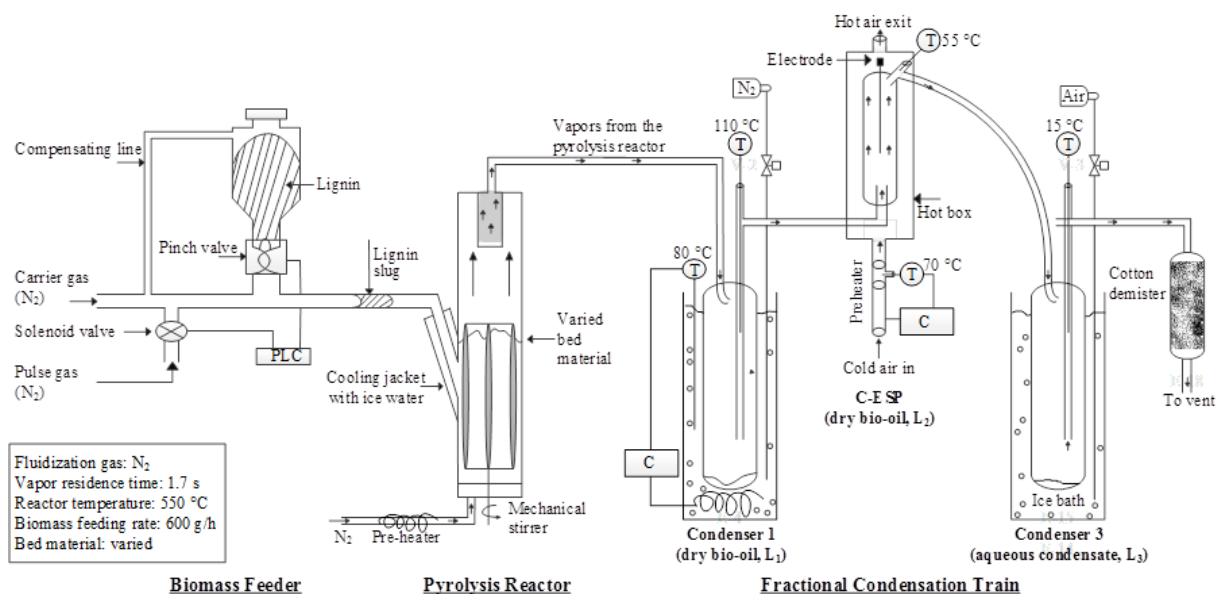
Figure 2.4: Fast Pyrolysis reactor, fluidized bubbling bed (Tumbalan-Gooty, 2014)

The fluidized bubbling bed reactor used for fast pyrolysis can be broken down into three main sections; the feeder, the reactor, and the condensation train. A schematic of the reactor setup is shown in Figure 2.4 (Tumbalan-Gooty, 2014).

The "slug injector" feeder (Berruti et al. 2013) was used to inject biomass into the reactor through a 45° line, 150 mm above the reactor bottom. The biomass which was held in an agitated hopper was discharged through a pinch valve that opened for 0.7 second every 5 seconds. This quick opening allowed for a slug of biomass to fall into the injector tube. This slug was then propelled into the reactor using an intermittent pulse of nitrogen as well as a continuous stream of nitrogen carrier gas. The opening of the pinch valve and pulse of nitrogen were synchronised using a programmable logic controller. The flow rate of carrier gas was controlled and monitored by a needle valve and Omega flow meter. The flow of pulse gas was calculated using the volume and pressure of a buffer tank and the pulse frequency (Berruti et al., 2013).

The reactor, a cylindrical tube, was made out of Inconel® 600 with a 78 mm internal diameter and a height of 580 mm, giving a total reactor volume of 2.79 L. Nitrogen, used as a fluidisation gas, entered through a gas distributor at the bottom of the reactor while carrier and pulse gas entered the reactor with the biomass via the injection tube. Silica sand was used as the bed material.

The reactor was heated by an induction heater that is capable of providing 2.5 to 12 kW of power. The induction system was normally controlled by an on-off controller to maintain a constant bed temperature, but could also be controlled manually to supply a constant power. Three K-type thermocouples were located along the vertical axis of the reactor to ensure the desired temperature was achieved in both the fluidised sand bed and the freeboard section of the reactor. The reactor temperatures and fraction of time that the heater is on were recorded using software created using the LabWindows™/CVI platform (National Instruments, Austin, TX).

The condensation train consists of a hot cyclonic condenser (condenser 1), a hot precipitator-cum-condenser (C-ESP), a cold cyclonic condenser (condenser 3), and a cotton wool demister (see Figure 2.4). Condenser 1 was submerged in a temperature-

controlled oil bath at 80 ᵒC to condense the heavy vapour components. The C-ESP was kept in a hot box maintained at 70 ᵒC. The C-ESP served two purposes: (1) to further condense the heavy vapour components, and (2) to collect aerosols via electrostatic precipitation. The ESP was maintained with an applied voltage of 9 kVDC. Condenser 3 was submerged in an ice bath to condense any remaining vapours in the vapour-gas stream. The gases then passed through the cotton demister to catch any remaining aerosols. This allowed for dry oil (< 1wt% water) to be collected in Condenser 1 and C-ESP while losing less than 10 wt% of the organics to Condenser 3 (Tumbalan-Gooty, 2014). For a more detailed description on the design, functionalities, and operation of the condensation train see (Tumbalan-Gooty, 2014).

2.3.2   Fast Pyrolysis Experimental Methods

In all experiments, 1500 g of silica sand with a Sauter-mean diameter of 70 μm and an apparent particle density of 1430 kg/m^3 was used as a bed material. Before each experiment the desired reaction temperature was selected and the combined gas flow rate of fluidisation, carrier, and pulse gases was adjusted to give a nominal vapour residence time of 1.7 seconds. The condensers and C-ESP were preheated and the C-ESP set to 9 kVDC. Once the entire system reached steady state the biomass was fed. After the run everything was cooled back down to room temperature before product collection.

Char yield was determined by weighing the combination of char and silica sand bed material at the end of each run. Oil yield was calculated by weighing Condenser 1, C-ESP, Condenser 3, and the cotton filter before and after each run. Gas yield was calculated by difference.

2.4   Autothermal Pyrolysis Experimental Methods

With autothermal pyrolysis, combustion reactions were used to provide the heat required for pyrolysis. Electrical heating was, thus, used solely to compensate for heat losses, which are relatively important for a small reactor, with a large wall area to volume ratio. Autothermal pyrolysis was conducted using the same equipment that was used for fast pyrolysis with the addition of compressed air into the fluidisation gas as a source of oxygen, and a constant power applied from the induction heater, controlled manually

rather than using the on-off controller. Several testing runs were required before a complete autothermal pyrolysis run could be completed. These testing runs were necessary to determine 2 things: 1) the power that must be applied to compensate for reactor heat losses, and 2) the oxygen to biomass feeding ratio that was necessary to achieve autothermal operation.

To determine the power that must be applied to account for heat losses several steps were taken:

1. The desired reaction temperature was decided;
2. All conditions must be identical to what is required for a typical pyrolysis run at that temperature (bed material, fluidisation, carrier, and pulse gas flow rate);
3. With all reactor conditions set the induction heater was controlled manually to provide a constant power. The power was adjusted until the desired reaction temperature was maintained at a steady state.

To determine the oxygen to biomass ratio required:

1. Reactor conditions and induction power must be set as previously determined to account for heat losses;
2. Biomass was then fed into the reactor at a known flowrate. Compressed air flowrate was also monitored;
3. The biomass to oxygen ratio was then varied until the desired reaction temperature was maintained at steady state. The amount of oxygen was increased if the temperature was to low, and decreased if the temperature was too high;
4. The oxygen to biomass ratio that was required for steady state autothermal pyrolysis was recorded.

These processes may need to be repeated iteratively to account for changes in gas flow rates. An advantage with induction heating is its faster response, due the reduction in thermal inertia.

Once both the constant power required to account for heat losses and required oxygen to biomass ratios were known, a complete autothermal pyrolysis run could be completed.

The methods for an autothermal run are the same as described in the fast pyrolysis methods section with the only changes outlined above.

2.5 Methods to Determine the Enthalpy of Pyrolysis

To determine the enthalpy of pyrolysis, the reactor and induction heating system with an on- off controller as described in the fast pyrolysis section was used. The energy supplied to the reactor was calculated using the power setting of the induction heater and measuring the fraction of time that the heater is on, giving an average power.

The difference in average power applied when the reactor is at steady state at reaction temperature before biomass feeding, and during biomass feeding shows the additional power supplied to the reactor during pyrolysis. However, all of the additional power supplied during biomass feeding does not solely go towards the pyrolysis reaction. With an increase in the average power supplied from the induction, there is also an increase in the reactor wall temperature, and therefore an increase in the reactor heat losses.

Therefore, a method was devised to determine the enthalpy of pyrolysis where reactor heat losses could be more accurately accounted for.

The energy balance of the reactor at steady state before biomass feeding can be described by equation 1, where the energy supplied to the reactor is equal to the heat losses of the reactor

$$Q_{in} = Q_{loss} \quad \textbf{(1)}$$

During biomass feeding, the energy balance can be described by equation 2, where the energy into the reactor is equal to the sum of the heat losses and the energy required for the pyrolysis reaction

$$Q_{in} = Q_{Loss} + H_{Pyrolysis} \quad \textbf{(2)}$$

The enthalpy of pyrolysis is commonly calculated by subtracting equation 1 from equation 2 using the assumption that the heat losses for both scenarios are equal. However, with additional power supplied to the reactor to provide the energy for

pyrolysis, there is an increase in the reactor wall temperature and therefore a corresponding increase in reactor heat losses. This leads to an overestimation of the enthalpy of pyrolysis.

This study used a new method where water was injected into the reactor, using a syringe pump, under the same experimental conditions as biomass feeding. The reactor energy balance under these conditions can be described by equation 3 where the energy in is equal to the reactor heat losses plus the enthalpy required to bring water from a liquid at room temperature to steam at reactor temperature.

$$Q_{in} = Q_{Loss} + H_{water} \quad \textbf{(3)}$$

The flow rate of water was adjusted until the fraction of time on, recorded through data acquisition, was the same as that recorded during biomass pyrolysis. With the same fraction of time on, the heat losses of equation 2 and 3 could be assumed equal, with greater certainty. With this assumption and the known thermodynamic properties of water equations 2 and 3 become a system of two equations with two unknowns that could be solved for the enthalpy of pyrolysis.

2.6 Product Analysis

Pyrolysis yields in this thesis were found to be highly reproducible, and careful control and monitoring of process conditions allowed for experimental errors or equipment malfunctions to be easily detected and the results discarded. Table 2.4 shows an example of the reproducibility of the pyrolysis yields from the slow pyrolysis of digestate at 550°C. These results were found to be highly reproducible especially considering the heterogenous digestate feedstock. This is due to the efficient mixing that occurred during the preparation of the feedstocks as well as the careful control and monitoring of the pyrolysis process conditions.

Table 2.4: Example of Reproducibility for Slow Pyrolysis of Digestate at 550°C

	Char Yield	Oil Yield	Gas Yield
Run 1	31.7%	25.5%	42.9%
Run 2	31.3%	25.0%	43.8%
Run 3	30.0%	27.1%	42.9%
Standard Deviation	0.007	0.009	0.004

All analytical experiments as outlined in this section were performed in triplicate and the average results are presented in this thesis.

Higher Heating Values

Higher heating values (HHV) of the char and the bio-oil samples were measured following the ASTM D4809-00 standard method and IKA S200 Oxygen Bomb Calorimeter.

Water Contents

Bio-oil water contents were determined using a Karl Fischer Titrator V20. Water yield was calculated by multiplying the total oil yield by the water content. Dry bio-oil yields were determined by subtracting the calculated water yield from the total bio-oil yield.

Moisture Contents

Solids moisture contents were determined using a Mettler Toledo HB43-S Halogen Moisture Analyzer.

Elemental Analysis

Elemental analysis (C, H, N, S, and O) was carried out using a Thermo Fisher Scientific Flash EA 1112 series analyzer. Vanadium pentoxide was used in order to detect sulfur.

Proximate Analysis

Proximate analysis was used to show the amount of ash, fixed carbon and volatile matter contained in a sample. Proximate analysis was completed according to ASTM D1762 – 84. Samples were dried in an oven at 105 ^oC. After drying the muffle furnace was heated to 950 ^oC and the samples were placed in the furnace in a covered crucible for 11 minutes to determine volatile matter. Samples were cooled in a desiccator and ashed at 750 ^oC for 6 hours. Fixed carbon content was calculated on a weight basis by subtracting the moisture, volatile, and ash components from the initial sample weight.

Gas composition

Product gas composition was determined using a Varian Micro-GC. The Micro-GC was calibrated with standard gas mixtures before every run.

Metals analysis

Metals leached from the char and biomass sample were determined by inductively coupled plasma mass spectrometry (ICP-MS).

Leaching

Leaching of heavy metals and nutrients from biomass and char samples was carried out using a Soxhlet extractor. Leaching refers to the extraction of a certain material from a solid to a liquid through percolation. Soxhlet extractors are capable of continuously washing the sample with fresh solvent while using a relatively small solvent quantity. The Soxhlet extractor can be separated into 3 parts: the boiling flask, the extraction chamber, and the condenser (see Figure 2.5). The boiling flask is used to boil the solvent, ensuring only fresh solvent evaporates. This solvent then bypasses the extraction chamber and enters the condenser. The condenser condenses the solvent where it is then deposited into the extraction vessel. Within the extraction vessel there is a cellulose thimble filled with the sample being washed. The solvent collects in the extractor vessel flooding the sample as it is washed. Once the level of the solvent reaches a certain height, a siphon

tube empties the extractor vessel and returns the used solvent with the extracted components to the distillation flask.

These leaching experiment were based off of EPA Method 3540C (EPA, 1996) for extracting compounds from solids such as: soils, sludges, and wastes using a soxhlet extractor. Where the methods in this thesis differ is in the choice of solvent and extraction time. Rather than using chemical solvents such Toluene and Methanol, deionized water was used as the extraction solvent to simulate rainfall and the real world condition that the biochars would be exposed to if applied to agricultural land. In Method 3540C the extraction time is specified between 16 to 24 hours in the experiments carried out in this thesis the soxhlet was left to operate for 24 hours for the digestate samples, and 72 hours for the sewage sludge samples. The longer time frame for the sewage sludge samples was used since the long term leachability of heavy metals was of a higher concern. The heater power was kept constant to ensure a constant flowrate of evaporated solvent. Two soxhlet extractors can be seen in operation in Figure 2.6.
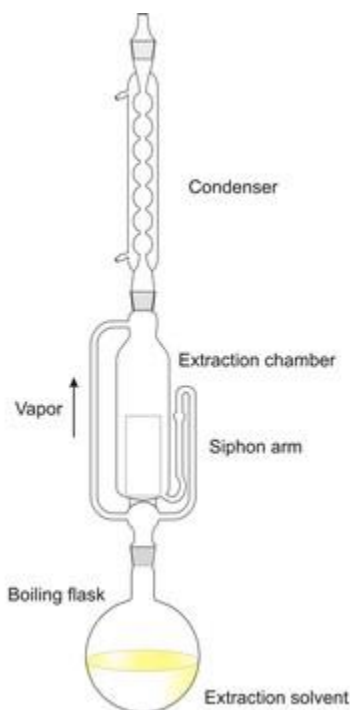
Figure 2.5: Diagram of Soxhlet Extractor (Generalix, 2014)
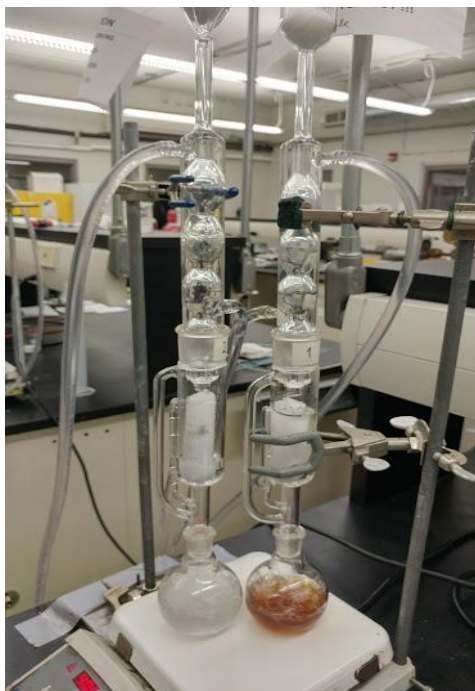
Figure 2.6: Two Soxhlet Extractors during operation.

Chapter 3

3   Results and Discussion

3.1   Digestate Pyrolysis

3.1.1   Effect of slow, fast, and autothermal pyrolysis and pyrolysis temperature on bio-oil properties

As shown in Figure 3.1, the yield of batch slow pyrolysis bio-oil increases with an increase in temperature. The yield of slow pyrolysis bio-oil increases from 13 to 43 wt% from 250 to 400 °C and remains relatively constant as temperatures increases beyond that point. A 2% decrease in the bio-oil yield from slow pyrolysis can be seen between 500 and 550 °C. This is counterintuitive since it represents a cumulative yield and should not decrease with increasing temperature. The decrease can be explained by the vaporisation of a small fraction of the condensed liquid caused by the hot product gases passing through the condenser. The total bio oil yield from the continuous operation of both fast and autothermal pyrolysis were lower than the yield achieved by slow pyrolysis. The total fast pyrolysis yield increases from 400 to 500 °C, while the autothermal pyrolysis yield remains relatively constant between the two temperatures.

The real difference between the three types of pyrolysis can be seen when looking at Figure 3.2 which shows the yield of dry bio-oil components. The dry-oil yield of slow pyrolysis shows the same trend as its whole oil yield with the largest increases between 250 and 400 °C with little change seen as temperatures increase beyond that point. The fast pyrolysis dry oil yield is shown to increase with respect to temperature and is significantly higher than the dry oil yield from slow pyrolysis. The dry oil yield from autothermal pyrolysis is lower than the yields seen for fast pyrolysis. This is due to a fraction of the dry oil components being combusted to supply the energy for the pyrolysis reaction. At 400 °C the yield of dry oil from autothermal pyrolysis is similar to that of slow pyrolysis but, as the temperature increases to 500 °C, the dry oil yield for autothermal pyrolysis was found to be between those for fast and slow pyrolysis.
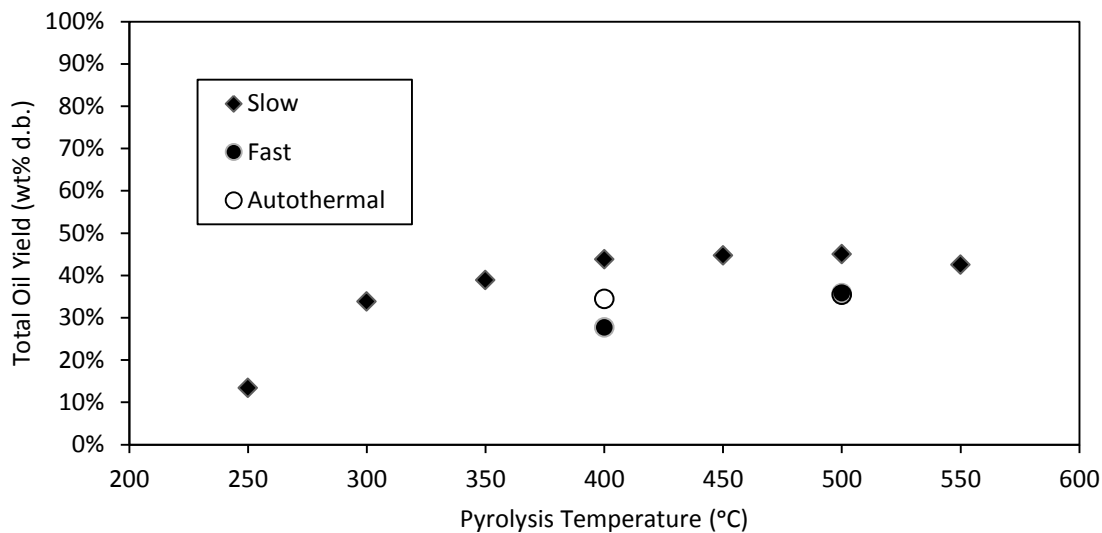
Figure 3.1: Total bio-oil yields from slow, fast, and autothermal pyrolysis of digestate vs pyrolysis temperature

Figure 3.2: Dry Bio-Oil yield of slow fast, and autothermal pyrolysis of digestate vs pyrolysis temperature

Figure 3.3 shows the higher heating values (HHV) of the dry oil sample. The HHV of slow pyrolysis dry bio-oils remains relatively constant at around 16 MJ/kg for all pyrolysis temperatures. The dry bio-oils from fast and autothermal pyrolysis had almost twice the heating value of the slow pyrolysis oils. Interestingly the dry bio-oils from autothermal pyrolysis had higher heating values than those from fast pyrolysis. This is most likely due to the combustion of the lighter, more volatile, components with lower heating values being combusted to provide the energy for the pyrolysis reaction.

Figure 3.4 shows the energy recovered in the bio-oil product. As expected slow pyrolysis showed poor energy recovery in the bio oil product. The energy recovery in the fast pyrolysis bio-oil increases with temperature and is maximised with fast pyrolysis at 500 °C. The energy recovery in the bio-oil from autothermal pyrolysis is between the values found for slow and fast pyrolysis. This can be expected due to the higher heating value, but reduced yield from partial combustion during autothermal conditions.

Figure 3.3: Heating Value of Dry Bio-Oil from slow, fast and autothermal pyrolysis of digestate vs pyrolysis temperature
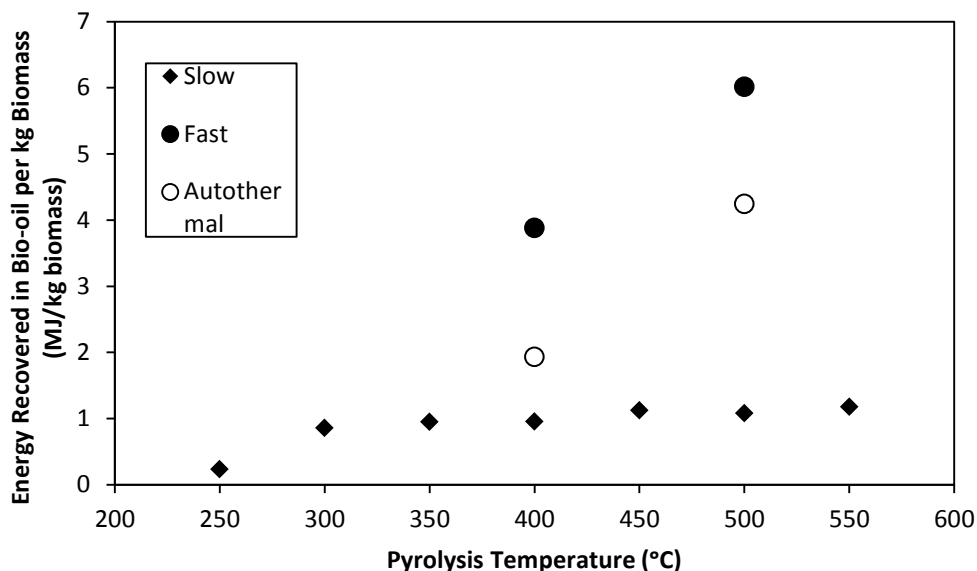
Figure 3.4: Energy Recovered in dry Bio-oil of slow, fast, and autothermal pyrolysis of digestate vs pyrolysis temperature

3.1.2   **Effect of slow, fast, and autothermal pyrolysis and pyrolysis temperature on biochar properties**

Figure 3.5 shows the biochar yield for slow, fast and autothermal pyrolysis vs. pyrolysis temperature. In all cases the biochar yield decreases with an increase in pyrolysis temperature. This is due to the increased volatilization of the biomass toward liquid and gas components at higher temperatures. The biochar yield for slow pyrolysis decreased from 66 to 28 % over the range of 250-550 °C. The yield of fast pyrolysis biochar was nearly identical to that of slow pyrolysis within the same temperature range. Under autothermal conditions, the yield of biochar was found to decrease with respect to slow and fast pyrolysis conditions, at the same temperature. This is again due to the partial combustion of the biochar to provide the energy for pyrolysis.
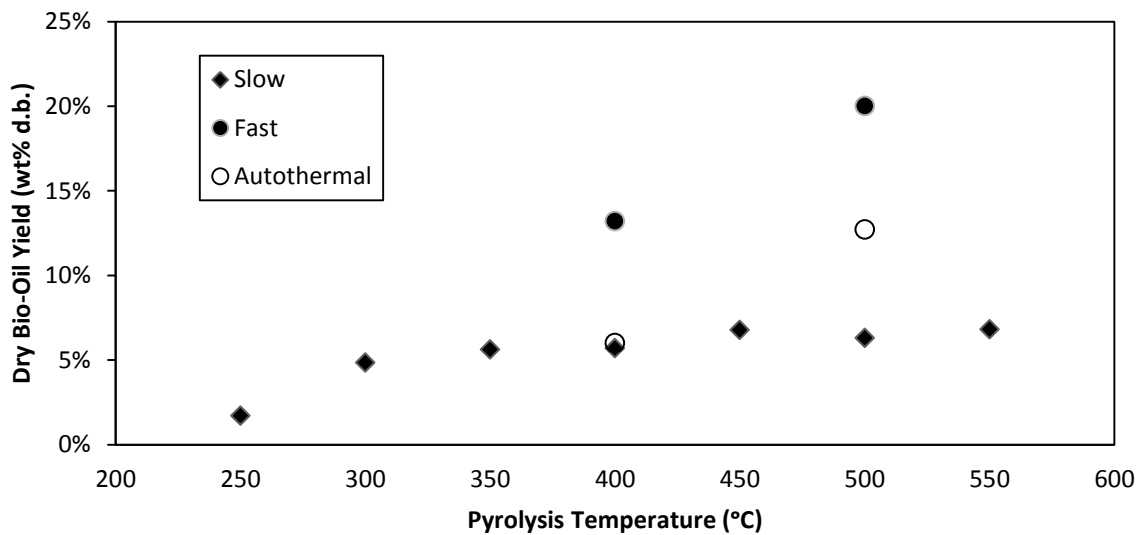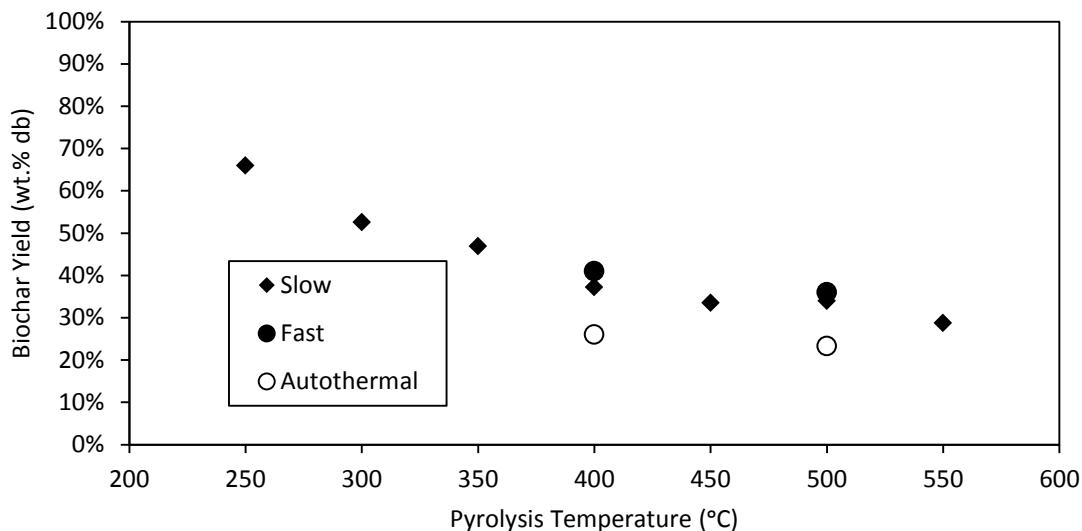
Figure 3.5: Biochar yield of slow, fast, and autothermal pyrolysis of digestate vs pyrolysis temperature

Figure 3.6 shows the heating value of slow, fast, and autothermal pyrolysis biochars vs pyrolysis temperature. Slow pyrolysis biochars had the highest heating values which increased with an increase in pyrolysis temperature. Slow pyrolysis biochars having the highest heating values is due to the increased residence time and therefore level of carbonisation that they achieve (see tables 3.1-3.3). The heating values of biochar from autothermal pyrolysis were higher than the chars made under fast pyrolysis conditions. This is due to the partial combustion of the more volatile organic fractions, containing hydrogen and oxygen, of the biochar during autothermal conditions (see tables 3.2 and 3.3, and figures 3.6). The combustion of these fractions of the char leaves a more carbonized, graphite like biochar with a higher heating value. This can be seen clearly in Figure 3.7 which shows the heating value of the biochars on an ash free basis.

Figure 3.8 shows the energy recovered in slow, fast, and autothermal pyrolysis chars per kg of biomass. For all pyrolysis types the energy recovery in the char decreases with an increase in pyrolysis temperature. Slow pyrolysis chars show the highest energy recovery followed by fast pyrolysis with autothermal pyrolysis giving the lowest energy recovery.

Again the lower energy recovery in the autothermal char can be explained by the partial combustion of the char during autothermal pyrolysis.
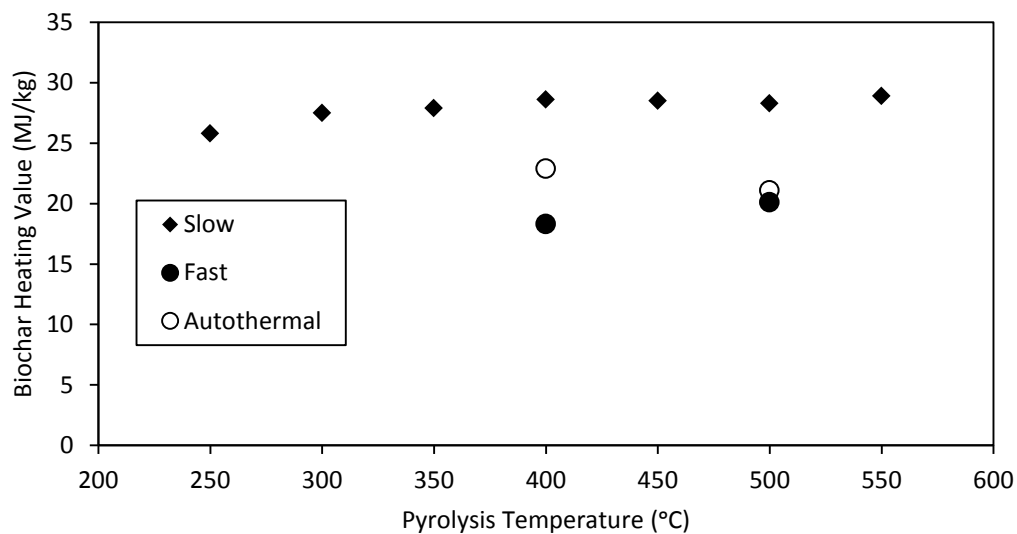
Figure 3.6: Biochar heating values from slow, fast, and autothermal pyrolysis of digestate vs pyrolysis temperature
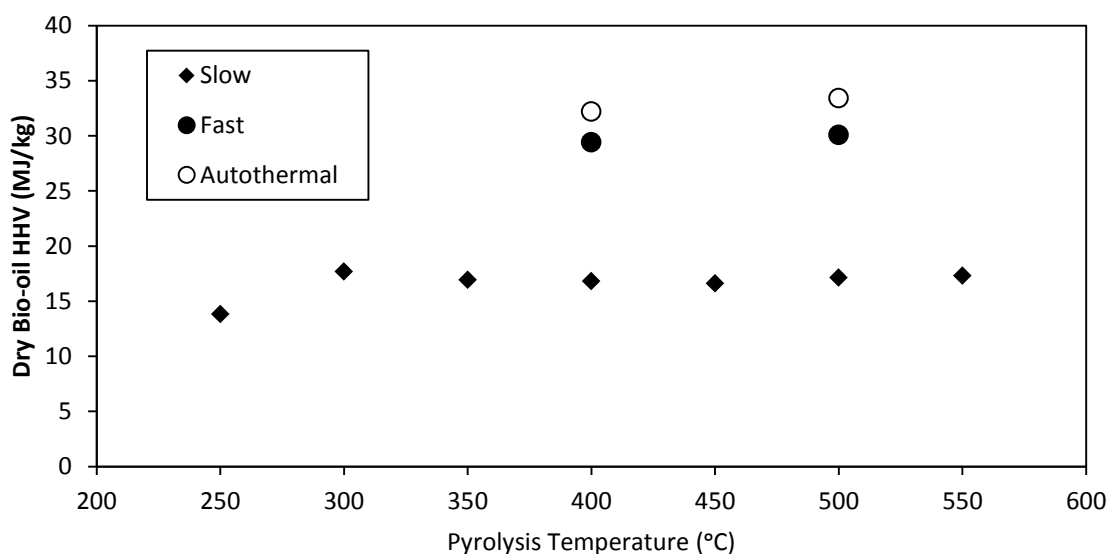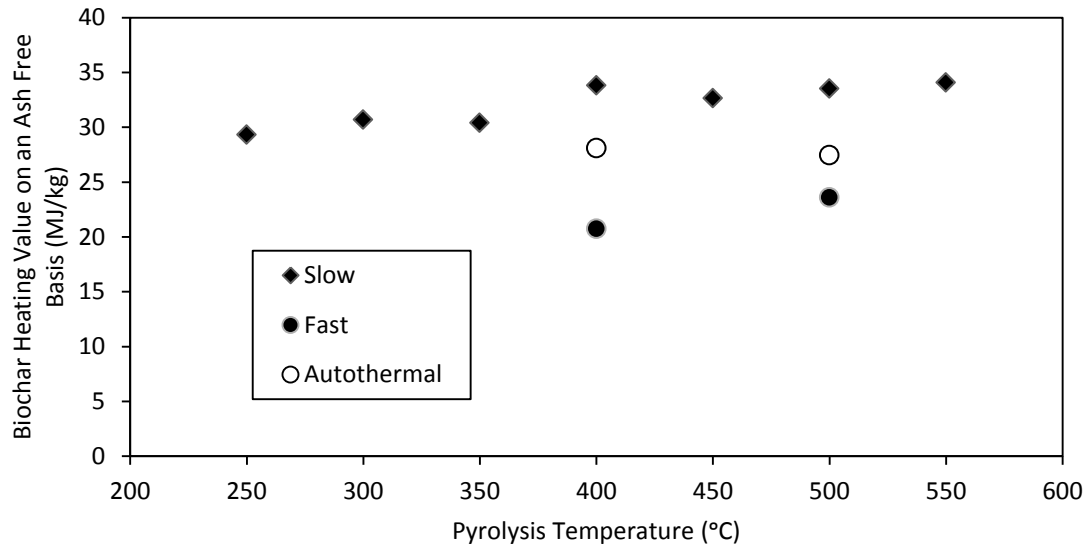
Figure 3.7: Biochar heating values on an ash free basis from slow, fast, and autothermal pyrolysis of digestate vs. pyrolysis temperature
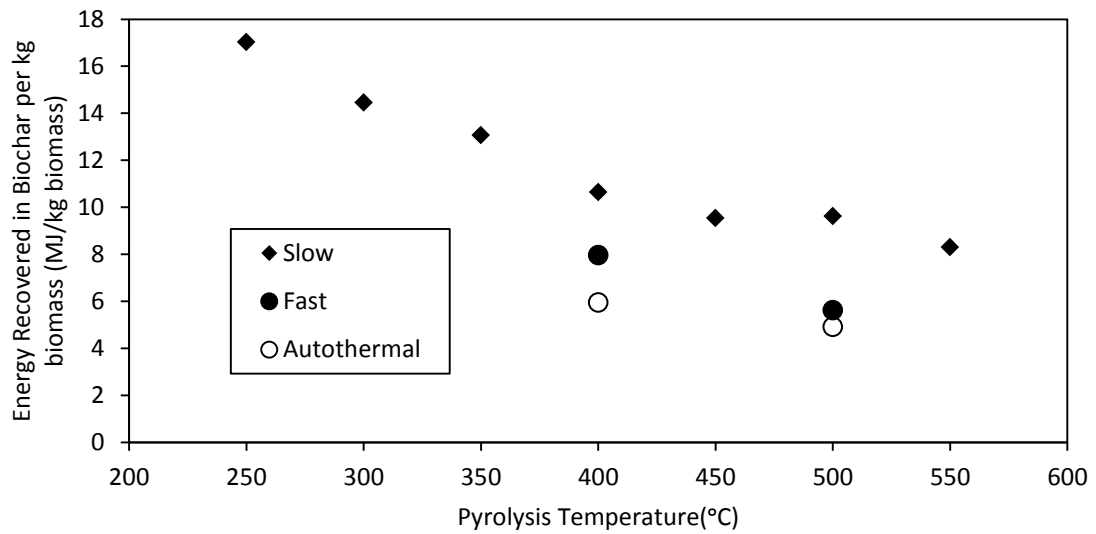
Figure 3.8: Energy recovered in biochar for slow, fast, and autothermal pyrolysis of digestate vs pyrolysis temperature

Table 3.1: Ultimate and Proximate Analysis of Slow Pyrolysis Biochars from Digestate

Pyrolysis Temperature (°C)	Ultimate Analysis (wt% d.b.)				Proximate Analysis (wt% d.b.)			Moisture (w.b.)
	N	C	H	O	Volatiles	Ash	Fixed Carbon	
0 (biomass)	2.5	46.5	5.6	40.0	84.5	5.4	10.1	6.7
250	2.3	63.0	5.4	17.3	62.2	12.0	25.8	2.1
300	2.9	63.0	4.8	18.9	47.1	10.4	42.4	3.4
350	2.4	67.6	4.0	17.8	41.4	8.2	50.4	4.0
400	2.4	67.1	3.6	11.5	32.9	15.4	51.7	3.8
450	2.9	74.3	2.8	7.3	23.4	12.7	63.8	4.0
500	2.3	71.2	1.6	9.3	22.2	15.6	62.2	5.8
550	2.8	76.0	1.8	4.2	20.2	15.2	64.6	5.3

Table 3.2: Ultimate and Proximate Analysis of Fast Pyrolysis Biochars from Digestate

Pyrolysis Temperature (°C)	Ultimate Analysis (wt% d.b.)				Proximate Analysis (wt% d.b.)			Moisture (w.b.)
	N	C	H	O	Volatiles	Ash	Fixed carbon	
400	2.0	56.0	2.4	27.8	34.9	11.8	50.3	5.8
500	1.9	61.7	2.4	19.2	28.9	14.8	59.3	8.8

Table 3.3: Ultimate and proximate analysis of autothermal pyrolysis biochars from digestate

Pyrolysis Temperature (°C)	Ultimate Analysis (wt% d.b.)				Proximate Analysis (wt% d.b.)			
	N	C	H	O	Volatiles	Ash	Fixed Carbon	Moisture (w.b.)
400	2.1	55.6	2.1	21.7	35.5	18.5	41.3	1.6
500	2.7	63.4	2.6	8.2	29.4	23.1	48.7	3.7
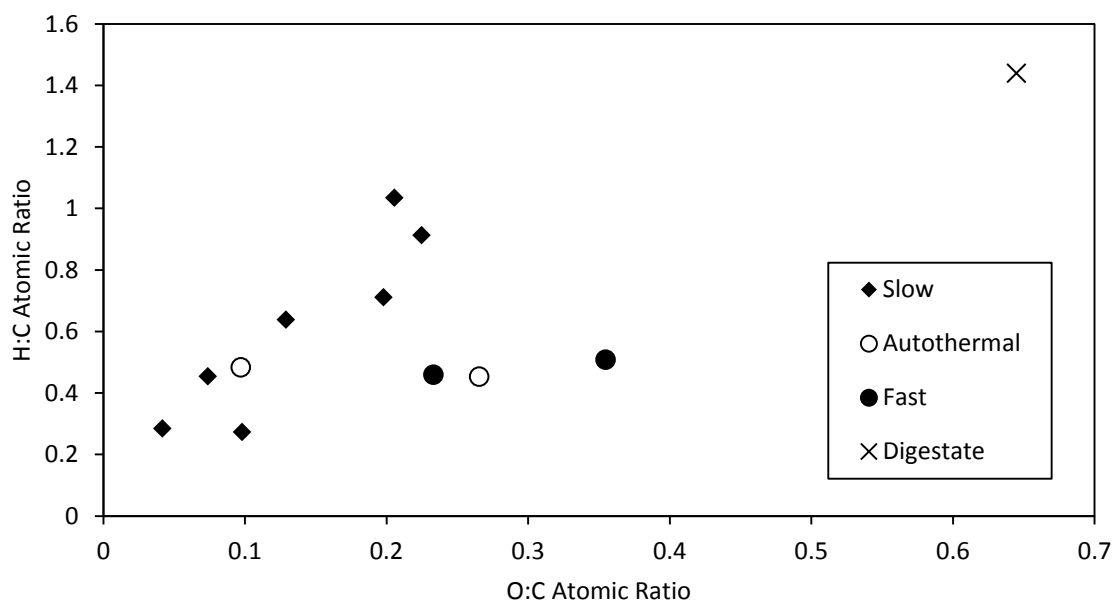
Figure 3.9: Van Krevelen Diagram for slow, fast, and autothermal pyrolysis biochars from digestate

The Van Krevelen diagram shown in Figure 3.9 is a graphical representation of the biochar's elemental composition and can be used to estimate its stability (Budai et al., 2013). Biochars are characterised in the Van Krevelen diagram by their H:C and O:C atomic ratios. Biochars with low H/C and O/C values are considered to be more graphite like materials and are expected to be more stable and less likely to degrade over time. Biochars with an O:C ratio of over 0.6 are expected to have a half-life of less than 100 years, biochars with an O:C ratio between 0.2 and 0.6 are expected to have a half-life between 100 and 1000 years, while biochars with an O:C ratio of less than 0.2 are expected to have a half-life of more than 1000 years (Spokas, 2010). In this diagram the chars produced at higher temperatures are found closer to the origin point whereas the biochars produced at lower temperature are found further away. Slow pyrolysis biochars produced at 400 ℃ and above as well as autothermal pyrolysis biochar produced at 500 ℃ were found to have O:C ratios below 0.2. All biochars have much lower O:C ratios than the biomass. This supports the possibility of using biochar as a carbon sequestration method.

3.1.3   Effect of slow, fast, and autothermal pyrolysis and pyrolysis temperature on leachability of nutrients from biochar

Figure 3.10 shows the leaching of the nutrient species; K, Ca, Mg, and P from slow pyrolysis chars. The leachability is shown as a ratio of the amount leached from the biochars to the amount leached from the digestate feedstock. This method was used to determine if pyrolysis conditions could be optimized to increase the leachability and recycling of desired nutritive species.

K was the only species to have an increased relative leachability after pyrolysis. The leachability also increased with an increase in pyrolysis temperature from 102 to 129%. Ca, Mg, and P, all showed reduced relative leachability when compared to the biomass feedstock. The leachability of Ca increased from 51-91% with an increase in temperature. This implies that these metals stay primarily in a water soluble form, and simply an increase in temperature could be utilized to increase the recyclability of K and Ca.

Mg leachability was reduced to below 75% for all pyrolysis temperatures although a strong trend with respect to temperature is not established. This indicates that the water soluble Mg found in the biomass has been transformed into organically bound forms through pyrolysis which are not water soluble. P leachability was lower than 25% for all pyrolysis temperatures and decreased to 10% at higher temperatures. This indicates that while the P in the biomass was likely in the form of water soluble phosphates these appear to be transformed into water insoluble compounds such as apatite or other phosphorous containing compounds (Bruun et al., 2017).
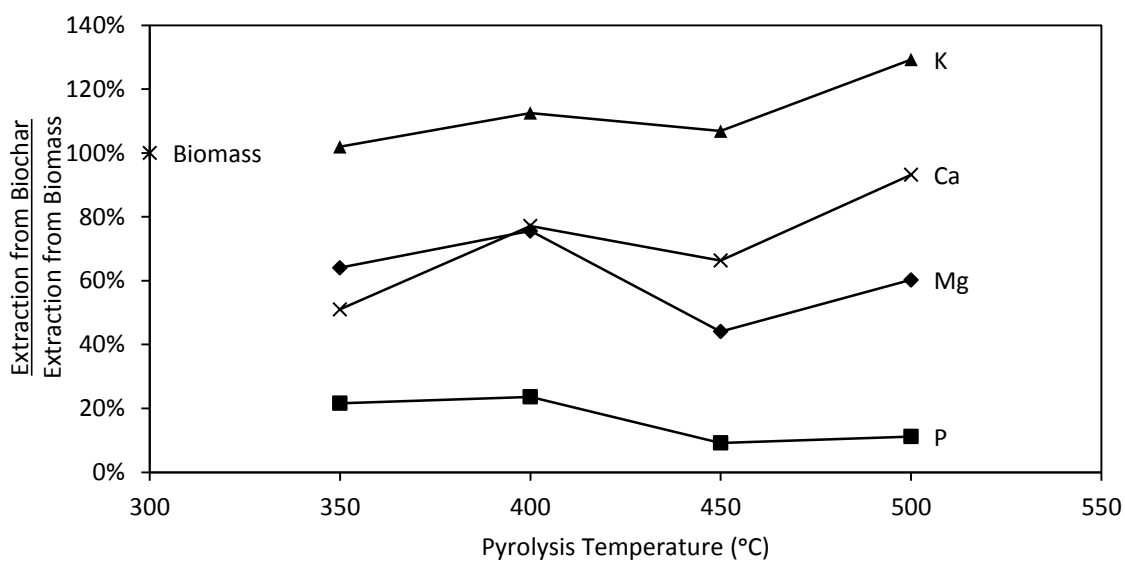
Figure 3.10: Effect of slow pyrolysis temperature on leachability of nutrients from digestate biochar

The difference in nutrient leachability of fast pyrolysis was also investigated. Figure 3.11 shows the percent change in leachability that occurs when switching from slow to fast pyrolysis. In general the leachability of the nutritive species from biochar is decreased under fast pyrolysis conditions. However, at 400 °C the leachability of Mg for fast pyrolysis biochar increased over that for slow pyrolysis biochar. This result is confirmed by (Kong, 2014) who found that the leachability of Mg from different biomass chars

could increase from slow to fast pyrolysis where the leachability of other metals decreased.

Nutrient leachability of biochars from autothermal pyrolysis was also examined. Figure 3.12 shows the percent change in leachability that occurs when switching from slow to autothermal pyrolysis. Like the biochars from fast pyrolysis, the biochars from autothermal pyrolysis had reduced leachability for nearly all metals and temperatures. The exception to this being P at a temperature of 500 °C. This exception can be explained by the low leachability of P and how a small increase in total leaching can result in a large relative increase.

The differences in leaching between the slow pyrolysis biochars and the biochars from fast and autothermal pyrolysis, which are produced at higher heating rates, are most likely explained by the differences in biochar chemical and morphological properties. Fast pyrolysis biochars have a higher oxygen content which would indicate a higher likelihood for these metals to become organically bound and less leachable in water (Kong, 2014). Another explanation is the morphological structure of fast pyrolysis biochars. Fast pyrolysis biochars undergo more significant morphological changes to the biochar structure than slow pyrolysis chars due to plastic deformation phenomena and the disappearance of fibrous structure of the biomass, leading to a more porous structure (Zhang et al., 2013). These changes could result in pores that are inaccessible by water or increase the pathway distance within the biochar particle to reach the outer char surface and the bulk fluid for extraction. The melted surface of the char could also cause changes in diffusivity of metals through the solid char material. These changes in the biochar physicochemical structure lead to inhibited mass transfer during leaching.
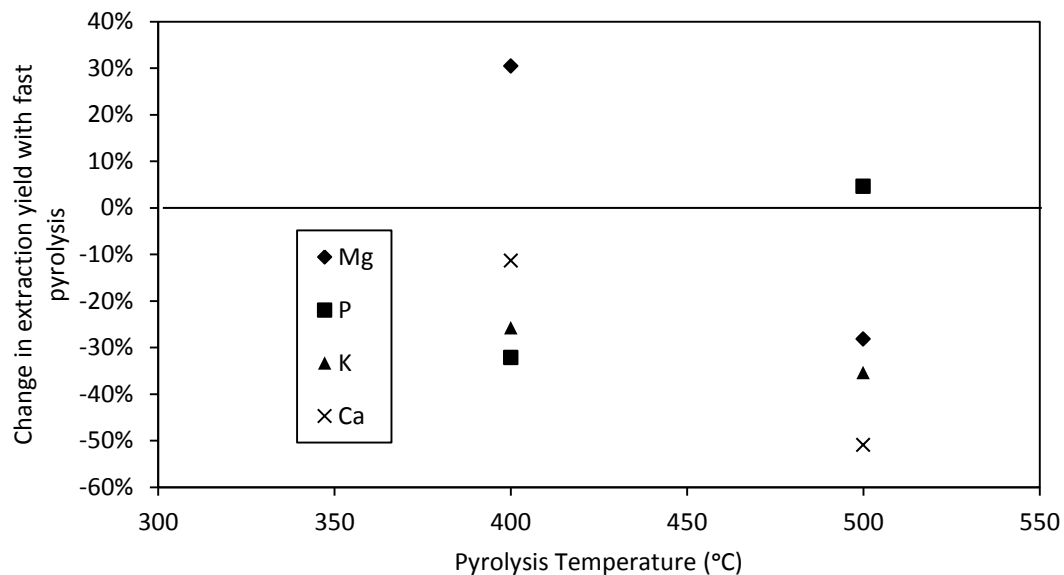
Figure 3.11: Change in nutrient extraction yield of digestate biochars from slow to fast pyrolysis
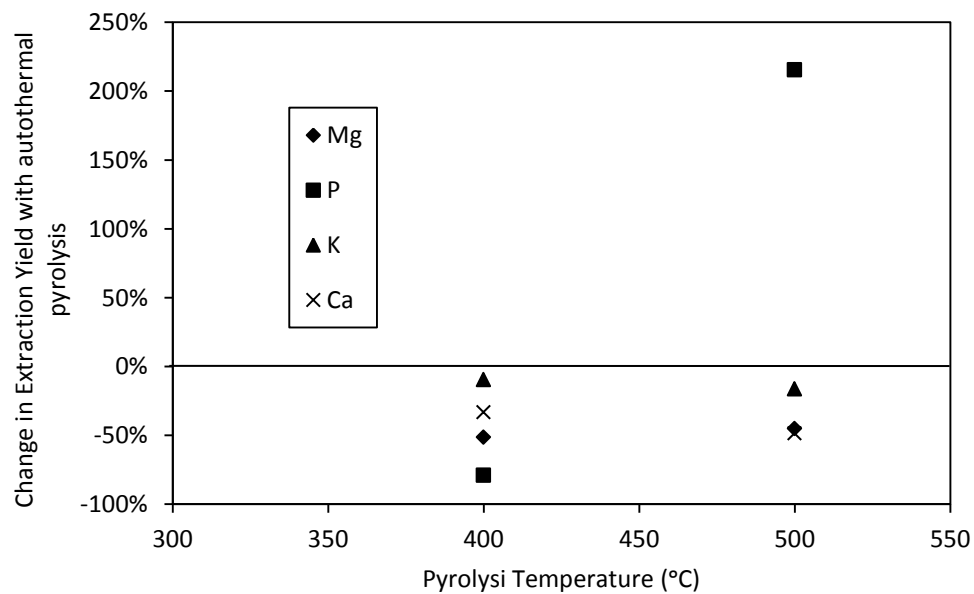
Figure 3.12: Change in nutrient extraction yield of digestate biochars from slow to autothermal pyrolysis

3.2 Sewage Sludge Pyrolysis

3.2.1 Effect of fast and slow pyrolysis and pyrolysis temperature on product yields

Figure 3.13 shows the effect of pyrolysis temperature on the product yields of slow and fast pyrolysis of sewage sludge. As the pyrolysis temperature increases the char yield decreases while the oil and gas yields increase. This is true for both slow and fast pyrolysis over the range of 300-500 °C. The total oil yields for slow and fast pyrolysis are nearly identical. The char yield decreases with a corresponding increase in the gas yield as you move from slow to fast pyrolysis.
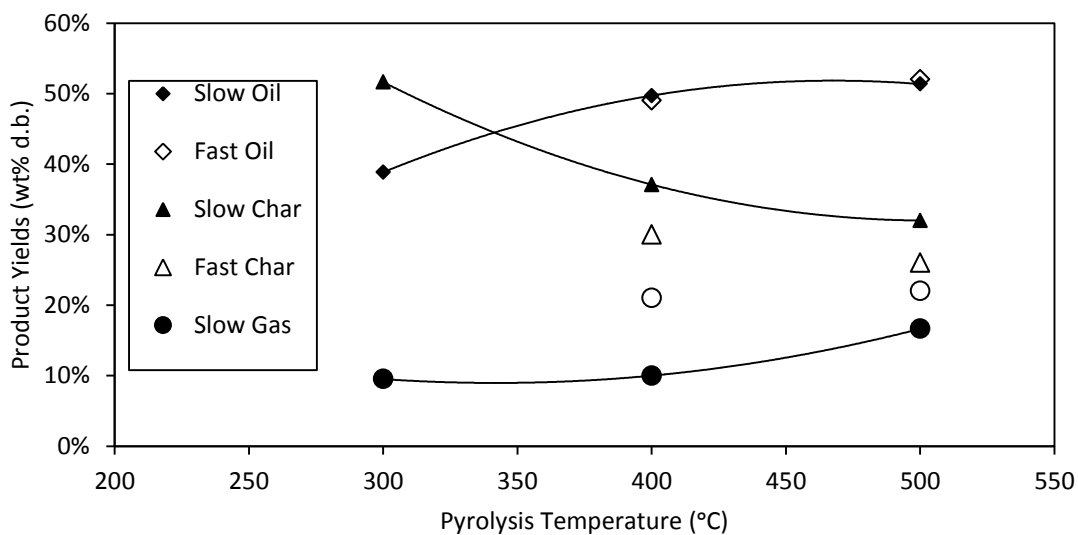
Figure 3.13: Product yields of fast and low pyrolysis of sewage sludge vs pyrolysis temperature with polynomial trend lines

3.2.2 Effect of slow and fast pyrolysis and pyrolysis temperature on bio-oil properties

The dry oil yield of fast and slow pyrolysis is shown in Figure 3.14. The dry oil yield for slow pyrolysis increases from 10% to 18% with an increase in pyrolysis temperature from 300 to 500 °C. The dry oil yield from fast pyrolysis is only nearly identical to that of slow pyrolysis. Figure 3.15 shows a similar trend with the dry oil heating values. The dry oil heating values rise with an increase in pyrolysis temperature and achieve a similar heating value to ethanol at the higher temperatures of 400 and 500 °C. The heating values are again similar for both slow and fast pyrolysis. Due to the similar yields and heating values the energy recovery in the oil is nearly identical for slow and fast pyrolysis as shown in Figure 3.16. The energy recovery in the oil is maximised at 500 °C with only a 4% difference between fast and slow pyrolysis. There is not a significant benefit for either slow or fast pyrolysis of sewage sludge with respect to bio-oil yield or energy recovery.
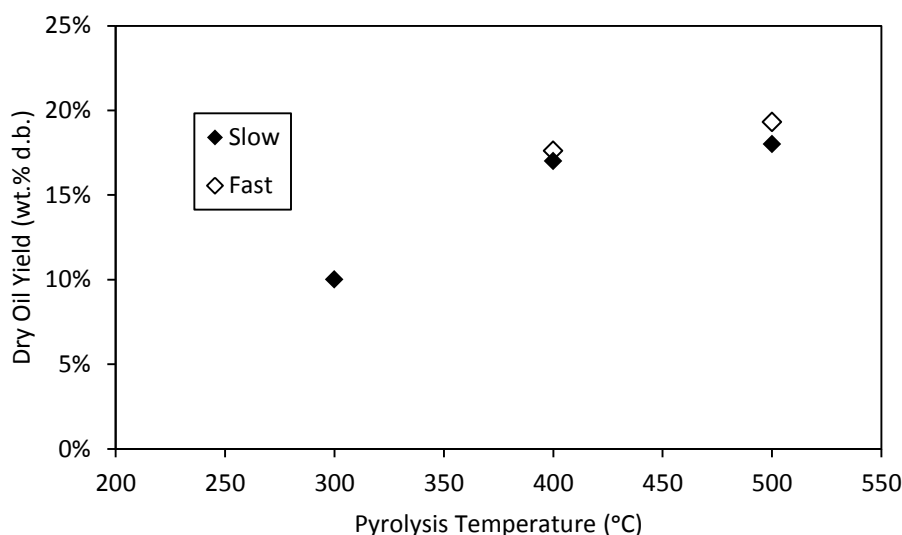
Figure 3.14: Dry bio oil yields of slow and fast pyrolysis of sewage sludge vs pyrolysis temperature
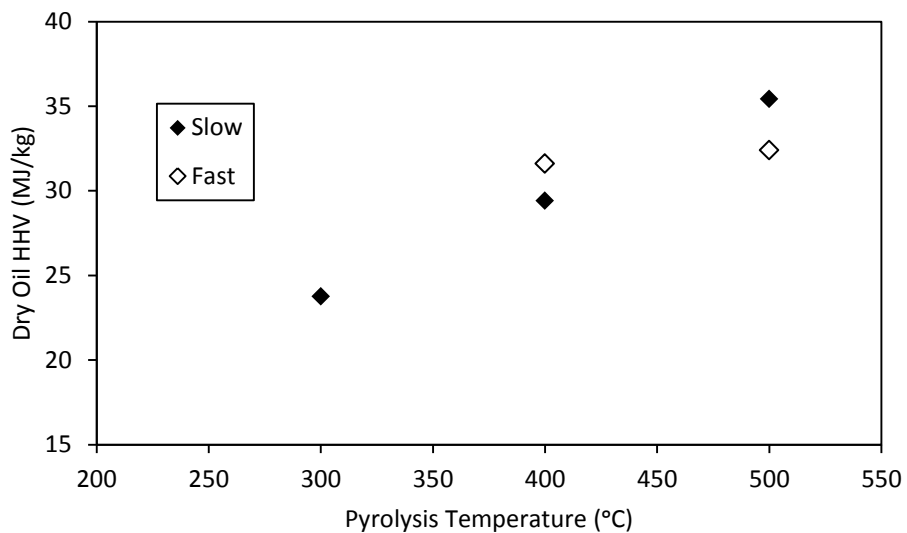
Figure 3.15: Heating values of dry bio oil from slow and fast pyrolysis of sewage sludge vs pyrolysis temperature
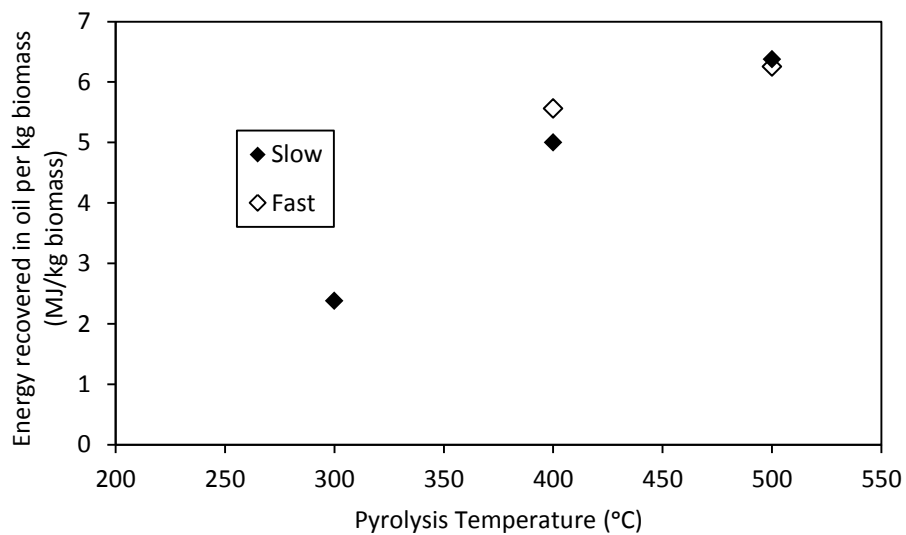
Figure 3.16: Energy recovered in bio-oil from slow and fast pyrolysis of sewage sludge vs pyrolysis temperature

3.2.3 **Effect of slow and fast pyrolysis and pyrolysis temperature on biochar properties**

The higher heating value of fast and slow pyrolysis biochars vs. pyrolysis temperature can be seen in Figure 3.17**.** The heating value of fast pyrolysis char is lower than that of slow pyrolysis char, which is due to the increased carbonization experienced during slow pyrolysis. What is interesting about this plot though is the decrease in biochar heating value with an increase in pyrolysis temperature. Typically the heating value of biochar will increase with an increase in pyrolysis temperature due to increased carbonisation. This decrease in heating value with an increase in temperature can be explained by the high ash content of sewage sludge and its chars. The increasing ash content (above 50%) at higher temperatures causes a negative impact on the heating value due to the lower amounts of combustible material. The increase in the biochar heating value on an ash free basis can be seen in Figure 3.18**.**

The energy recovery on the biochar is shown in Figure 3.19**.** The recoverable energy in the char decreases with an increase in pyrolysis temperature. Slow pyrolysis chars have a higher energy recovery due to their higher yield and heating values.
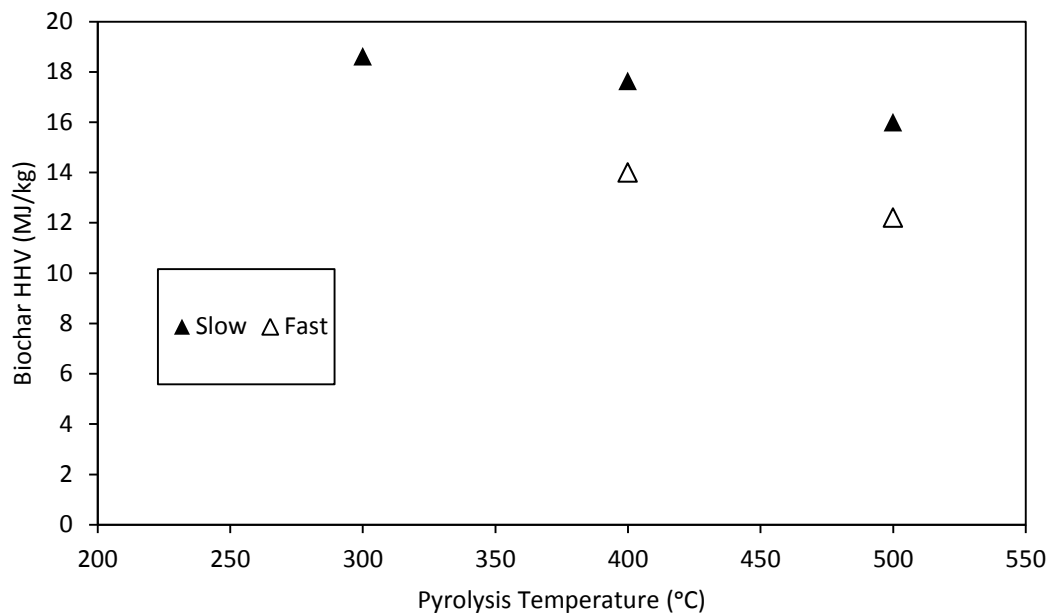
Figure 3.17: Heating values of biochar from slow, and fast pyrolysis of sewage sludge vs pyrolysis temperature
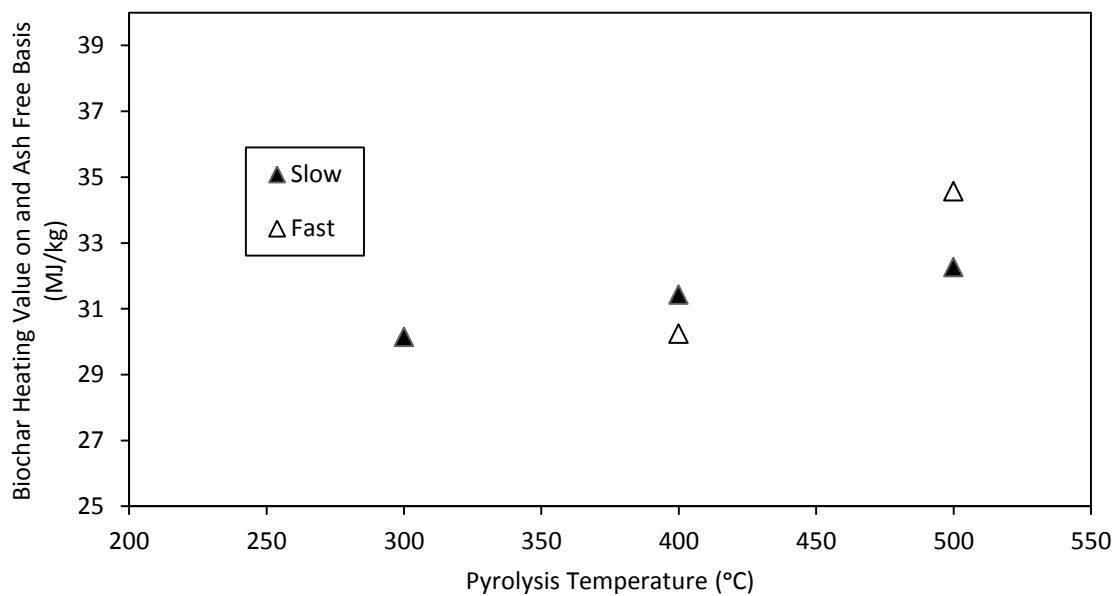
Figure 3.18: Heating values of biochar on an ash free basis from slow and fast pyrolysis of sewage sludge vs pyrolysis temperature
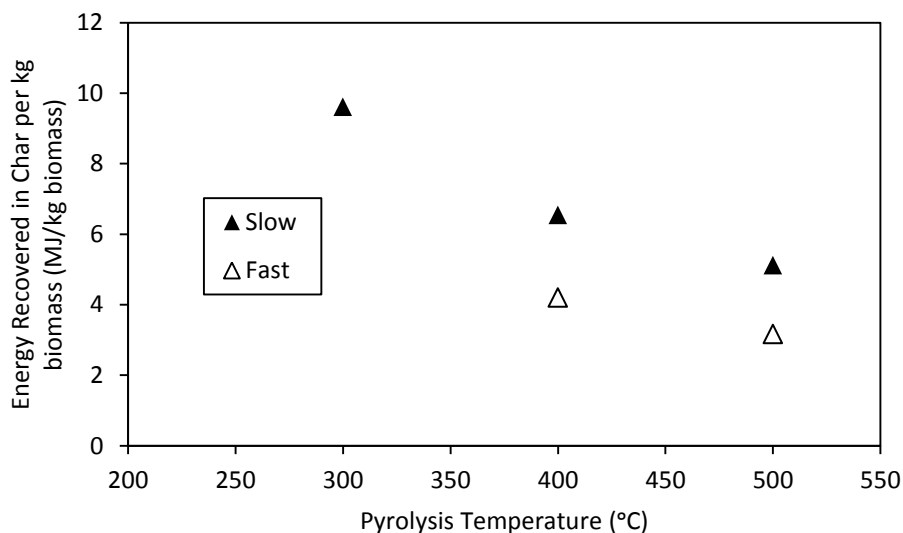
Figure 3.19: Energy recovered in biochar from slow and fast pyrolysis of sewage sludge vs pyrolysis temperature

Pyrolysis Temperature		Ultimate Analysis (wt% d.b.)				Proximate Analysis (wt% d.b.)			
		C	H	S	O	volatiles	ash	fixed carbon	Moisture
0 (Biomass)	3.4	38.3	5.0	<0.05	37.3	72.1	16.0	11.9	7.0
300 Slow	4.9	45.4	4.2	<0.05	7.3	49.8	38.3	11.9	2.6
400 Slow	4.6	42.1	3.2	0.6	5.6	38.3	44.0	17.7	0.0
500 Slow	5.7	40.5	2.0	0.7	0.7	26.0	50.4	23.7	3.0
400 Fast	4.3	29.9	2.4	1.3	8.4	35.5	53.7	10.7	3.5
500 Fast	3.8	23.4	1.5	1.9	4.7	25.8	64.7	9.5	3.6

Table 3.4: Ultimate and Proximate Analysis of slow and fast pyrolysis biochars from sewage sludge
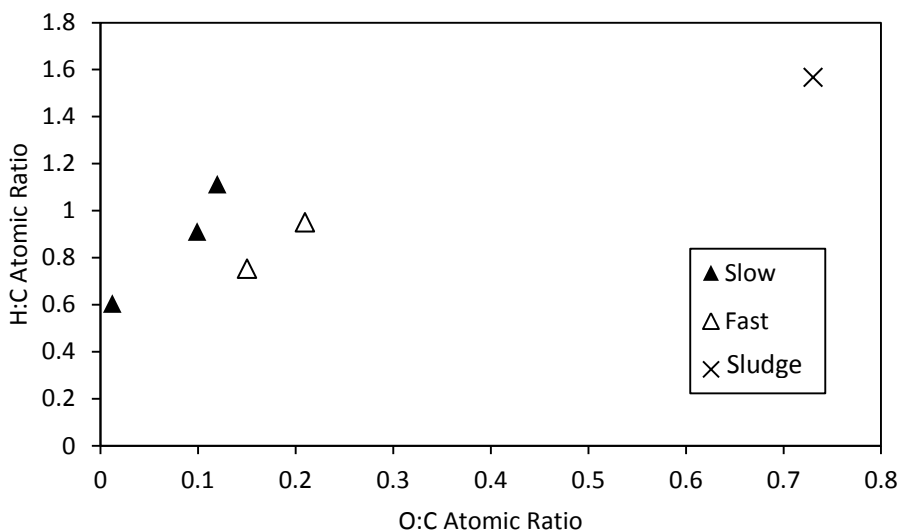
Figure 3.20: Van Krevelen diagram of slow and fast pyrolysis biochars from sewage sludge

The Van Krevelen diagram shown in Figure 3.20 shows that all biochars have a significant reduction in O:C ratio with respect to the raw biomass. All chars have an O:C ratio of 0.2 or less and can be expected to have a half-life of 1000 years or more. The biochars produced at higher temperatures are found closer to the origin point and are expected to be the most stable. Slow pyrolysis chars showed lower O:C ratios compared to fast pyrolysis chars. Based on this slow pyrolysis chars would be more beneficial for long term carbon sequestration due to their increased stability.

Table 3.5 shows the leaching rate of restricted and nutrient metals from slow and fast pyrolysis biochar produced at 500 °C. The leaching rate is defined as the percentage of metals present in the biochar that are leached out through soxhlet extraction with deionized water. The slow pyrolysis biochar showed leachability below the detection limits for the majority of the restricted metals with low leachability of copper and zinc. The slow pyrolysis biochar also leached 29% of the available K but very little of the phosphorous. The fast pyrolysis biochar showed roughly twice the leachability of the metals that were leached by the slow pyrolysis char. The fast pyrolysis char also saw

leaching of Cr, Mo, and Ni. This increased leaching is most likely due to the higher ash content and reduced carbon matrix of the fast pyrolysis char (see Table 3.4). This leads to more of the metals being accessible for leaching. Slow pyrolysis char showed better ability to reduce the leaching of heavy metals but also had reduced leachability of nutrient species. Fast pyrolysis had increased leachability of restricted metals, but due to their relatively low concentrations in the tested sludge the levels are still below regulated limits. The fast pyrolysis char also had increased leachability of potassium. From this analysis slow pyrolysis would be more attractive for sludge with higher heavy metal concentrations where reduced leachability is desirable, while fast pyrolysis would be more attractive for sludge with very low heavy metal concentrations where their leachability is not a concern and release of nutritive species should be maximized.

Table 3.5: leaching of metals from ash, slow pyrolysis biochar, and fast pyrolysis biochar derived from sewage sludge

Restricted Metal	Slow	Fast
Cd	None Detected	None Detected
Cr	None Detected	0.7%
Cu	1.1%	1.5%
Mo	None Detected	48.0%
Ni	None Detected	2.4%
Pb	None Detected	None Detected
Zn	0.2%	0.4%
Nutritive Metals		
K	29.0%	66.0%
P	0.2%	0.5%

3.2.4   **Energy Balance of Sewage Sludge Fast Pyrolysis**

To complete an energy balance for the fast pyrolysis of sewage sludge, a gas analysis for fast pyrolysis of sewage sludge at 500 °C was completed. 500 °C was chosen to complete the energy balance because it had the highest energy recovery in the gas and oil by-products that could be used to provide energy for the drying and pyrolysis of the sewage sludge. The gas product composition and energy recovery in the gas stream can be seen in Tables 3.6 and 3.7, respectively.

Gas Component	Weight %
CO*	43.4%
C_2H_4	37.5%
CO_2	13.9%
C_3H_8	3.9%
C_4H_{10}	1.3%

Table 3.6: Gaseous product components from fast pyrolysis of sewage sludge at 500 °C

Total Gas Yield	Heating Value (MJ/kg)	Energy in Gas per kg biomass (MJ/kg)
22%	24.7	5.4

Table 3.7: Heating Value and Energy recovery in gas stream of fast pyrolysis of sewage sludge at 500 °C

The enthalpy of pyrolysis was calculated by using the methods described in the materials and methods section. The enthalpy of pyrolysis for dry sewage sludge was found to be 2.2 MJ/kg. Figure 3.21 shows the energy required to pyrolyze 1 kg of dry sewage with respect to the sludge water content. Energy must be supplied both for the evaporation of water and for the pyrolysis reaction. This causes a significant increase in the required energy with an increase in water content of the sludge due to the high enthalpy of vaporization of water. Overlaid on the graph are the energy recovered from the oil and gas streams generated from the pyrolysis of 1 kg of biomass. The higher heating values of the oil and gas streams were used in this analysis. By utilizing only the gas stream to provide energy for the evaporation of water and pyrolysis reaction a theoretical maximum water content of 55 wt% could be accommodated in the sludge while maintaining a thermally self-sufficient process. If both the oil and gas streams are used to provide energy the theoretical maximum water content that can be accommodated is 78 wt%. This is promising since the average water content of dewatered sludge is 72 wt%. However, for true self-sustaining operation a thermal efficiency of 92% in the process must be achieved which is above the 87% reported efficiency for similar systems (Liu et al., 2017). Further developments in sewage sludge dewatering technology could greatly increase the efficiency and attractiveness of the pyrolysis process.
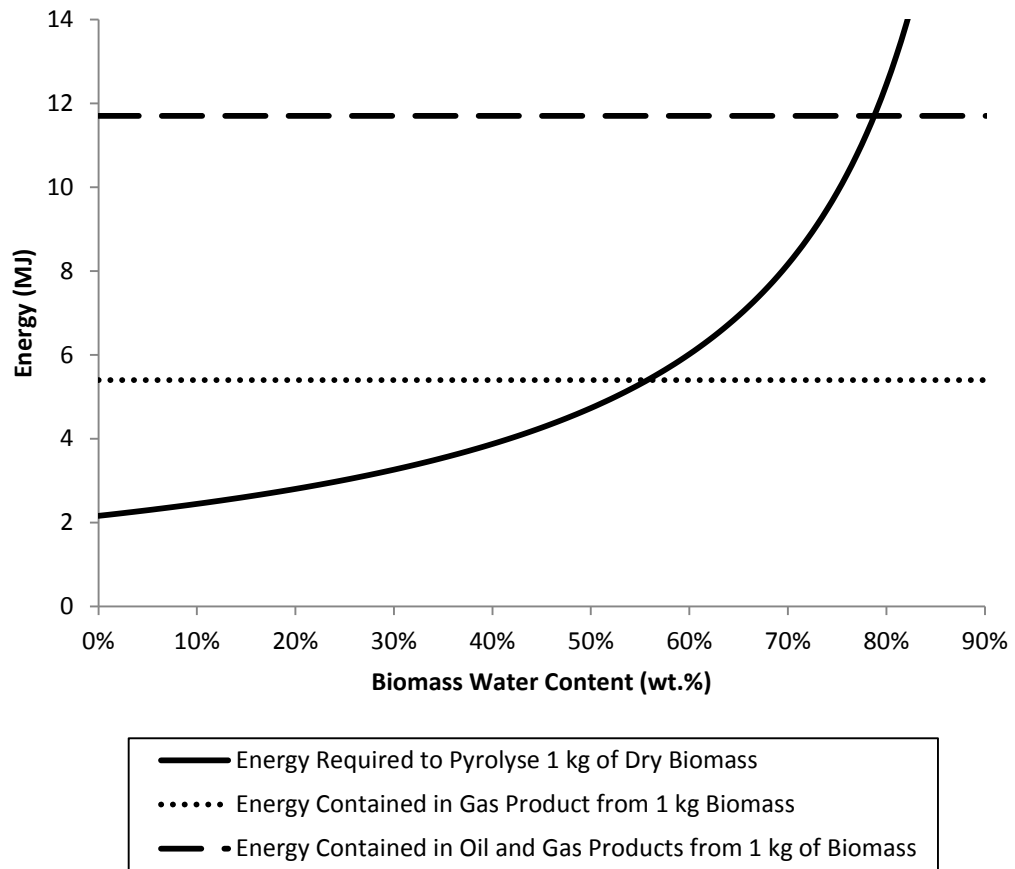
Figure 3.21: Energy required to pyrolyze 1 kg of sewage sludge vs sludge water content, balance with gas and oil by-products

3.2.5   **Sewage Sludge Pyrolysis Economic Assessment**

An economic model was developed for the slow pyrolysis of sewage sludge at 500 °C, with pyrolysis and sequential combustion of the vapour and gas products. The process consists of five main sections; sludge drying, pyrolysis, combustion of gases and vapours, gas cleaning, and char storage. The heat from combustion of the pyrolysis gases and vapours, along with assist fuel when needed, is used to provide the energy for the sewage sludge drying and pyrolysis stages. This method of using the combustion of the pyrolysis gases and vapours to provide energy for the process has been shown to provide stable and easy control of the process parameters. (Koga et al., 2007; Liu et al., 2018). A simple process flow diagram can be seen in Figure 3.22.
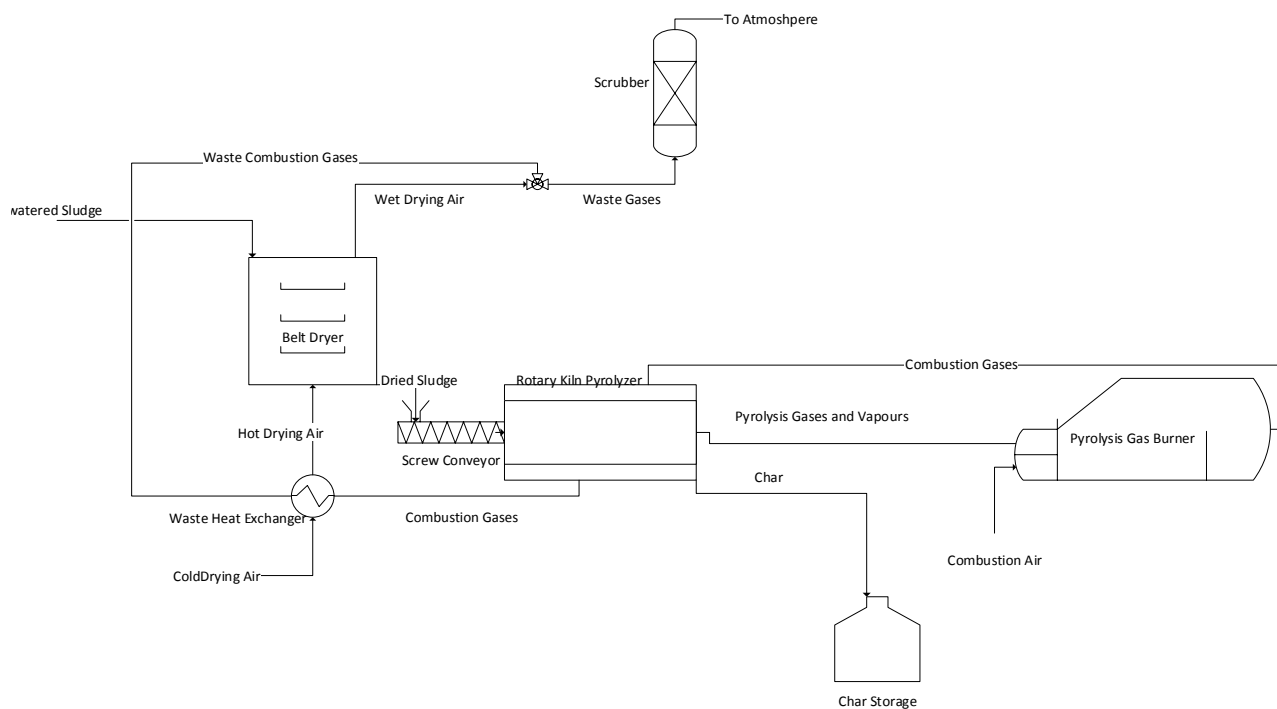
Figure 3.22: Process Flow Diagram of Sewage Sludge Pyrolysis for Economic Assessment

The economic model was developed as a study estimate, according to (Peters et al., 1991). The results shown are for a plant capacity of 2.1 tonnes/hr with 8 000 operational hours per year. Equipment capacities and sizing were determined by mass and energy balances from pyrolysis experiments. Purchased equipment costs were used in the following order of priority; quotations from manufacturers, published equipment costs, estimates from literature (Peters et al., 2002). Total capital and production costs were calculated using factored estimates from (Peters et al., 1991) along with energy balance data from pyrolysis experiments. The overall thermal efficiency of the process was assumed to be 87% based on tests performed by (Liu et al., 2017) on a similar pyrolysis and vapour combustion set-up. All dollar values are given in 2016 Canadian dollars. Cost

data was corrected using the Chemical Engineering Plant Cost Index (Chemical Engineering, 2017). If cost data was not available for equipment of the designed capacity it was corrected using the sixth tenth rule shown by equation 4.

$$Cost\ of\ equipment\ at\ sized\ b = \left(cost\ of\ equipment\ at\ size\ a\right) * \left(\frac{Size\ b}{Size\ a}\right)^{0.6} \quad (4)$$

The biochar product was assumed to have 0$ value considering current business practices in biosolids management provide the biosolids to end users for free (City of Ottawa, 2017).

A study estimate carried out in this matter is considered to have an uncertainty up to ±30% (Peters et al., 1991).

Economic Analysis Results

Tables showing the capital and production costs are below.

Table 3.8: Purchased Equipment Costs

Equipment Section	Purchased Cost
Belt Dryer	$631,000
Char Storage	$286,000
Pyrolysis Gas Burner	$488,000
Rotary Kiln Pyrolyzer	$1,500,000
Scrubber	$151,000
Total Purchased Equipment Costs	**$3,100,000**

Table 3.9: Direct Capital Costs

Direct Capital Costs

Expense	Cost
Installation	$1,200,000
Piping	$950,000
Instrumentation and Control	$797,000
Electrical Installation	$306,000
Building and Services	$888,000
Land and Site Development	$368,000
Utilities and service facilities	$1,690,000
Total	**$6,200,000**

Table 3.10: Indirect Capital Costs

Indirect Capital Costs

Expense	Cost
Engineering and Supervision	$920,000
Construction Expenses	$1,070,000
Contractor's fees	$612,000
Contingencies	$919,000
Total	**$3,500,000**

Table 3.11: Total Capital Investment Summary

Expense	Cost
Total Purchased Equipment Costs	$3,100,000
Direct Capital Costs	$6,200,000
Indirect Capital Costs	$3,500,000
Working Capital	$680,000
Total Capital Investment	**$13,500,000**

Table 3.12: Annual Direct Production Costs

Direct Production Costs

Expense	Cost
Labour Costs	$300,000
Utilities (electricity)	$325,000
Utilities (natural Gas)	$145,000
Maintenance and repair	$185,000
Operating Supplies	$30,000
Laboratory Expenses	$45,000
Total	**$885,000**

Table 3.13: Annual Indirect Production Costs

Indirect Production Costs

Expense	Cost
Overhead	$120,000
Insurance and Property Tax	$61,000
Total	**$181,000**

Table 3.14: Annual General Expenses

Annual General expenses

Expense	Cost
Administrative Costs	$30,000
Research and Development	$73,000
Distribution	$146,000
Total	**$249,000**

Table 3.15: Annual Total Operating Costs

Expense	Cost
Direct Manufacturing Costs	$885,000
Indirect Manufacturing Costs	$181,000
General Expenses	$249,000
Total Operating Costs	**$1,320,000**

Table 3.16: Net Present Value Summary

Total Capital Investment	$13,500,000
Annual Expenses	$1,320,000
Discount Rate	10%
Project Lifetime	20 years
NPV	**-$23,500,000**

Over a project lifetime of 20 years and a discount rate of 10% the Net Present Value of such a plant would be -$23.5 Million Dollars. However, this value would change if the biochar is considered a profitable product. The production costs of biochar were

determined to be $250 per tonne. That is the price at which the revenues from sale of biochar would equal annual expenses. Another benefit of the pyrolysis process is the avoided costs from landfilling of the sewage sludge ash. Assuming a tipping fee of $72 per tonne additional avoided costs of $195 000 per year could be achieved.

3.2.6 Life Cycle Assessment of Sewage Sludge Pyrolysis and Incineration

3.2.6.1 Goal and Scope

The goal of this life cycle assessment (LCA) is to compare the relative environmental impacts of pyrolysis and incineration of sewage sludge from the Greenway Wastewater Treatment Plant in London, Ontario. The results will inform decision makers in the industry of potential environmental benefits of pyrolysis as an emerging sewage sludge treatment option. A total of four scenarios will be examined:

1) Incineration with no energy recovery and landfilling of ash
2) Incineration with Organic Rankine Cycle (ORC) energy recovery and landfilling of ash
3) Slow Pyrolysis at 500 °C with application of biochar to agricultural land
4) Slow Pyrolysis at 500 °C with char used as coal substitute in cement kiln and ash used as a cement filler

The functional unit, the reference to which all flows are related, is 9918 kg of dewatered sewage sludge with a water content of 72 wt%, or 2777 kg of sewage sludge on a dry basis. This is the amount of sludge required to produce 1 tonne of biochar.

OpenLCA, created by GreenDELTA, an open source LCA software was used to create the models for each scenario. European reference Life Cycle Database of the Joint Research Center was used as the life cycle assessment database. CML Baseline 2015 is used as the life cycle impact assessment method, the impact categories examined are global warming potential over 100 year timescale (GWP100) and freshwater ecotoxicity.

3.2.6.2 System Boundary

Figures 3.23 and 3.24 show the system boundaries for the incineration and pyrolysis processes respectively. The impacts were examined during operation only. The impact of manufacturing and decommissioning of capital equipment was not examined. The impact

from the operation of the wastewater treatment plant was not included since it is the same for all scenarios.
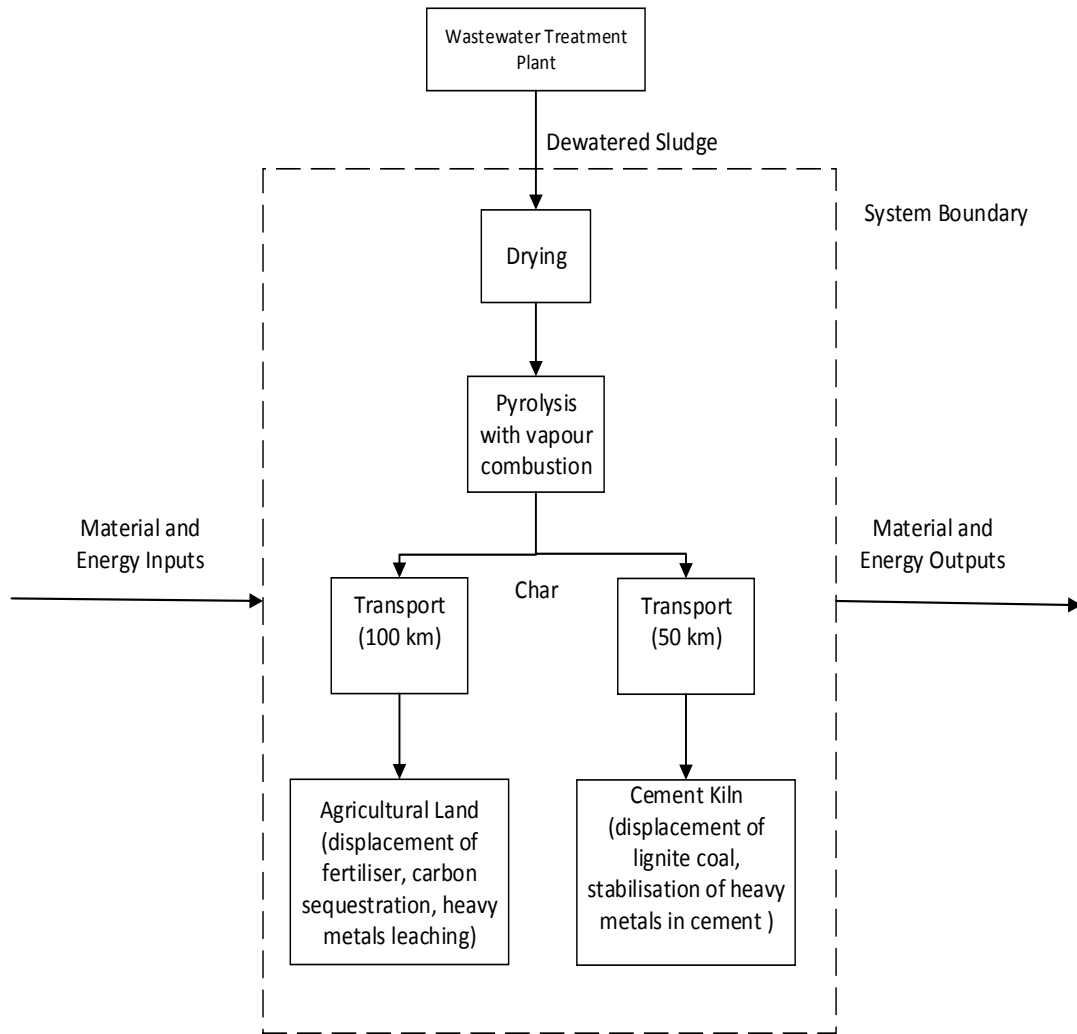
Figure 3.23: LCA Pyrolysis Options System Boundary
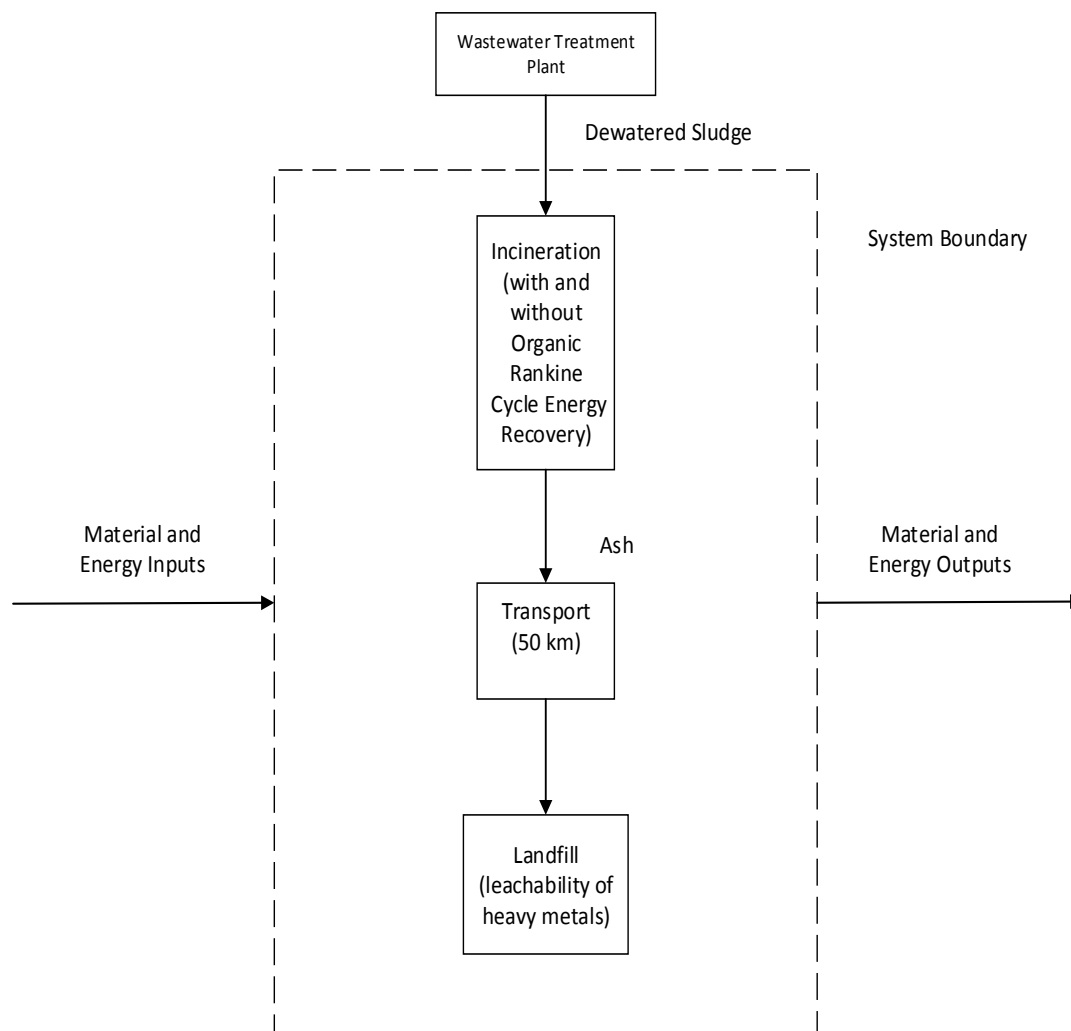
Figure 3.24: LCA Incineration Option System Boundary

3.2.6.3   **Life Cycle Inventory**

For each scenario an inventory of energy and material inputs and was created. These flows were determined using energy, mass and species balances determined during pyrolysis experiments, as outlined in this thesis, and from operation and emission reports from the City of London (City of London, 2017.)**.** Sewage sludge was considered to be carbon neutral in all scenarios.

Transportation distances were considered to be 50 km for the incineration and pyrolysis with use of ash in a cement kiln options; and 100 km for application of the biochar to

agricultural land. In the application of biochar to agricultural land option the stability and carbon sequestration of the biochar is a benefit to the system. The potassium and phosphorous that are leachable from the char are also considered a benefit since they can displace the mineral fertilizers of potassium chloride and triple superphosphate. Leachability of heavy metals has a negative impact to the system. Other potential benefits from adding the biochar to agricultural land such as reduced greenhouse gas emissions from the soil were not included.

In the use of biochar in a cement kiln scenario both the displacement of lignite coal and stabilisation of heavy metals from using the ash as a cement filler benefit the process.

In the incineration without energy recovery no energy recovery from the incineration gases is accounted for. Therefore even though no emissions come directly from the sewage sludge incineration all other aspects of the process contribute negatively. For incineration with Organic Rankin Cycle energy recovery the heat from the incinerator gases is transformed into electric power, replacing electricity from the grid, creating a benefit for the system.

3.2.6.4   Life Cycle Impact Assessment
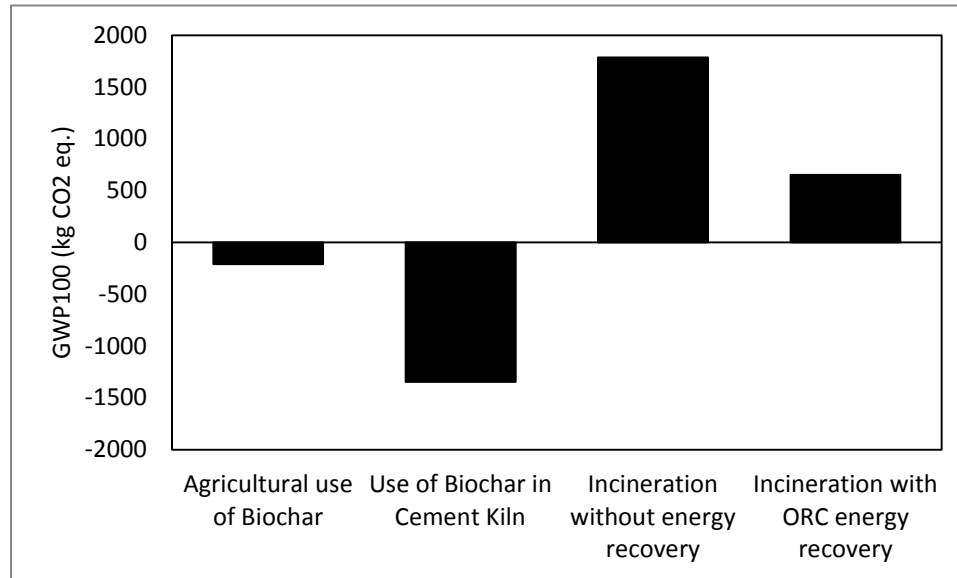
Figure 3.25: LCA Global Warming Potential Results
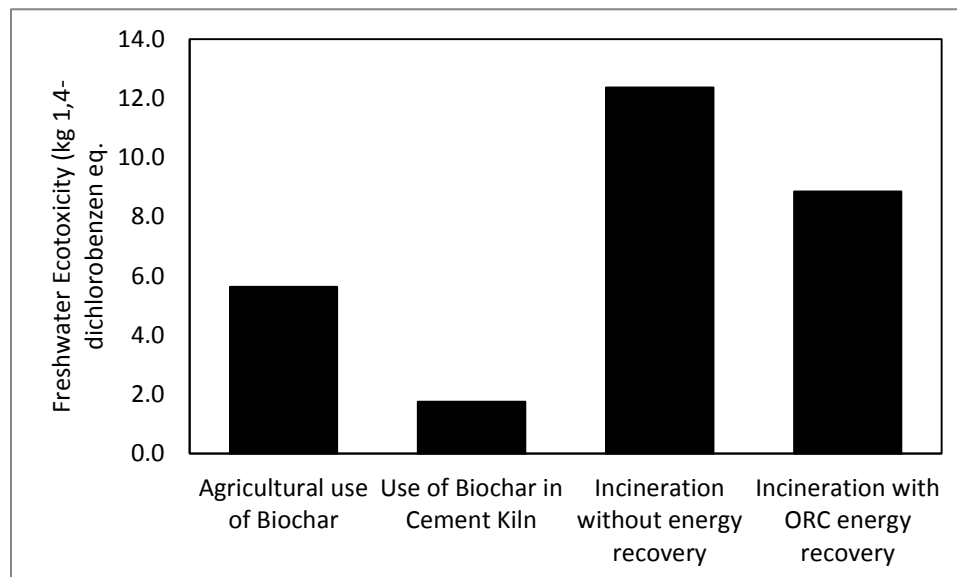
Figure 3.26: LCA Freshwater Ecotoxicity Results

Figure 3.25 shows the LCA results for global warming potential in kg CO_2 eq. Incineration without energy recovery showed the worst results, followed by Incineration with Organic Rankine Cycle energy recover, use of biochar on agricultural land, and use of biochar in a cement kiln showing the best results. Incineration without energy recovery has the worst impact due to no aspect of the process creating greenhouse gas reductions with each step of the process contributing to its total global warming potential. Incineration with ORC energy recovery shows considerable improvement over incineration without energy recovery. The ORC cycle is able to create excess electricity in a carbon neutral manner which can replace standard grid electricity. Agricultural land application of the biochar shows a decrease in global warming potential. This is accomplished by recycling the energy in the vapour and gas streams within the pyrolysis process, decreasing demand for fossil fuels, displacement of mineral fertilisers, as well as carbon sequestration in the biochar. The carbon in the biochar was assumed to be stable over the 100 year time horizon for the global warming potential due to its low O:C ratio. Use of the biochar in a cement kiln showed the highest reductions to the global warming potential. This is due partially to the reuse of energy in the pyrolysis process, but primarily due to the replacement of lignite coal as a fuel. No other reduction has the same impact on global warming potential as the replacement of lignite coal with a carbon neutral fuel. This supports the work in Japan of using carbonized sewage sludge as a coal replacement in traditional coal fired power plants (Oda, 2007).

Figure 3.26 shows the LCA results of freshwater ecotoxicity in kg 1,4 dichlorobenzene eq. The order of impact from best to worst was the same as for the global warming potential. The impact is highest for incineration without energy recovery due to zero realized reductions in utility demands and the leachability of heavy metals from the ash. The impact for incineration with ORC energy recovery is lower than that without energy recovery. This is due to the production of electricity decreasing demand on the electric grid, however large differences are not seen since the primary source of the freshwater ecotoxicity is the leachability of the heavy metals present in the ash. More significant reductions are seen with the pyrolysis option with biochar application to agricultural land.

This is due to the decreased leaching of heavy metals from the biochar. Again the lowest impact is seen with biochar used in a cement kiln. With the ash from the cement kiln being used as a cement filler, there is no opportunity for the leaching of heavy metals. This combined with the replacement of lignite coal as a fuel source creates the largest reduction in toxicity.

Overall, the two pyrolysis scenarios performed better than the incineration scenarios with respect to the impact categories of global warming potential and freshwater ecotoxicity. This is mainly due to the beneficial properties of the biochar including, low leachability of heavy metals, carbon stability, and potential as a solid fuel.

3.3 Comparison of Digestate and Sewage Sludge Pyrolysis

For slow pyrolysis, the dry bio-oil yields and heating value were higher for sewage sludge than the digestate. However, under fast pyrolysis conditions the dry oil yield and heating value of the digestate oil increased significantly and is comparable to that achieved by fast pyrolysis of the sewage sludge. This is particularly true at the higher pyrolysis temperature of 500 ℃. Sewage sludge does not experience a similar increase in dry bio-oil yield and heating value when going from slow to fast pyrolysis. Digestate also experiences higher biochar yields on an ash free basis when compared to sewage sludge. These differences are likely due to the difference between lignocellulosic and non-lignocellulosic biomass; specifically the high lignin content of the digestate feedstock (Ahring et al., 2015).

The higher biochar yield experienced by the digestate feedstock can be explained by the lower level of decomposition that lignin experiences compared to other biomass fractions such as cellulose and hemicellulose. At temperatures up to 500 ℃ cellulose almost completely decomposes and hemicellulose decomposes to 20 % of its initial mass. At the same temperature lignin shows fairly little decomposition and retains approximately 60 % of its initial mass (Burhenne et al., 2013). This lower amount of decomposition results in an increased biochar yield for digestate.

The difference in bio-oil yields can be explained by the higher lignin content of digestate and the resultant higher vapour residence times for slow pyrolysis of digestate. The biomass components of hemicellulose and cellulose decompose relatively rapidly between the temperatures of 225-325 °C and 325-375 °C respectively. Lignin, on the other hand, decomposes gradually between 200 and 500 °C. When biomass with a high lignin content is processed under the slow pyrolysis conditions used in this study the instantaneous vapour flow rate is relatively low throughout the entire reaction resulting in longer vapour residence times within the reactor. These longer vapour residence times promote further cracking of the vapour products to water and gas products. The slow evolution of volatiles also increases the amount of secondary reactions between the volatile vapours and the char. The slow reaction rate results in the released volatiles taking a longer time to escape the biochar matrix. With the increased contact time, the volatiles react with the biochar matrix forming water, gases, and secondary char through cracking and repolymerisation reactions respectively (Bridgwater et al., 2007; Nanda et al., 2016). These secondary cracking reactions are minimized during fast pyrolysis where the biomass is rapidly heated, increasing the rate at which the volatiles leave the biochar matrix. Fluidization and carrier gas also control the vapour residence inside the reactor to minimize further cracking of the volatile products. This results in higher dry bio-oil yields during fast pyrolysis.

Sewage sludge being a non-lignocellulosic biomass is a more complex and varied feedstock containing proteins, carbohydrates, and lipids. These components do not undergo the same thermochemical decomposition process as traditional lignocellulosic biomass (Li et al., 2017). Although the thermochemical conversion mechanisms of these components are not as well known, it is shown that they are not as thermally stable as lignin which can explain the lower ash-free biochar yield experienced by the sewage sludge (Magdziarz et al., 2014). It also appears that under fast pyrolysis conditions further decomposition of the biomass solids takes place when compared to slow pyrolysis with a corresponding increase in the gaseous product yield. This is either due to the direct conversion of the solids to light gaseous product or secondary cracking of produced vapours to gaseous products.

Overall, the differences in the product slates for the pyrolysis of anaerobic digestate and sewage sludge is due to the different composition of the feedstocks. The varying compositions result in differing reaction mechanisms and kinetics resulting in different product compositions.

Chapter 4

4 Conclusions

In this thesis the potential for pyrolysis of solid anaerobic digestate and municipal sewage sludge was successfully studied.

Fast pyrolysis at higher temperatures (500 °C) was preferred for the production of bio-oil with a high heating value. Slow pyrolysis produced the best biochar in terms of yield, heating value, and stability. Stability and heating value of biochar on an ash free basis was found to increase with an increase in pyrolysis temperature. Autothermal pyrolysis decreased the yield of bio-oil and bio-char products but increased their quality. This is potentially attractive for large scale pyrolysis units.

Leachability of heavy metals and nutritive species from the biochar depended on the metal and feedstock being examined. However, trends can be seen based on pyrolysis conditions for each feedstock. These trends are dependent on the inherent physicochemical properties of the biochar products. Potassium was found to have good leachability from the digestate slow pyrolysis biochars. Heavy metals were found to be stabilised in the slow pyrolysis biochars from sewage sludge.

An economic analysis for a sewage sludge pyrolysis plant processing 2.1 tonnes of dry solids per hour was developed. An environmental life cycle assessment determined that pyrolysis of sewage sludge, with use of the biochar as a substitute fuel in a cement kiln, had the least impact on global warming potential and fresh water ecotoxicity of examined scenarios.

Some new experimental methods were also developed for the completion of this thesis. A new method for the accurate measurement of the enthalpy of pyrolysis was developed. Soxhlet extraction with deionized water was determined to be a quick and economical method for leachability measurements.

Chapter 5

5   Recommendations

In this study Soxhlet extraction of pure char samples was used to determine the effect of pyrolysis conditions on the leachability of nutritive species and heavy metals from the biochar products. However, these leaching characteristics could change when the char is added to soil. It is recommended that Soxhlet extraction of char samples mixed with soil be completed to investigate the effect of soil properties on the leaching characteristics. Changes to the pH of the extraction water and its effects on leachability would also be of interest. A fundamental study into the mechanisms of char leaching could also be of interest. By better understanding the leaching mechanisms, biochars that are engineered to promote the leachability or stability of certain metals could be produced.

Autothermal pyrolysis was also determined to be feasible for the pyrolysis of anaerobic digestate. Scaling up the autothermal pyrolysis process to a reactor with a lower surface area to volume ratio and therefore lower proportionate heat losses would be of interest. At larger scales additional energy to compensate for heat losses may not be necessary.

A new method for measuring the enthalpy of pyrolysis was developed in this thesis. Using this method to create a database for various feedstocks could provide valuable information to the pyrolysis research community.

Bibliography

Abiven, S., Schmidt, M. W. I., & Lehmann, J. (2014). Biochar by design. *NATURE GEOSCIENCE Www.nature.com*, *7*. https://doi.org/10.1038/ngeo2154

Agrafioti, E., Bouras, G., Kalderis, D., & Diamadopoulos, E. (2013). Biochar production by sewage sludge pyrolysis. *Journal of Analytical and Applied Pyrolysis*, *101*, 72–78. https://doi.org/10.1016/j.jaap.2013.02.010

Ahring, B. K., Biswas, R., Ahamed, A., Teller, P. J., & Uellendahl, H. (2015). Making lignin accessible for anaerobic digestion by wet-explosion pretreatment. *BIORESOURCE TECHNOLOGY*, *175*, 182–188. https://doi.org/10.1016/j.biortech.2014.10.082

Amutio, M., Lopez, G., Aguado, R., Artetxe, M., Bilbao, J., & Olazar, M. (2012). Kinetic study of lignocellulosic biomass oxidative pyrolysis. *Fuel*, *95*, 305–311. https://doi.org/10.1016/j.fuel.2011.10.008

Andreattola, G., & Foladori, P. (2006). A Review and Assessment of Emerging Technologies for the Minimization of Excess Sludge Production in Wastewater Treatment Plants. *Journal of Environmental Science and Health, Part A*, *41*(9), 1853–1872. https://doi.org/10.1080/10934520600779026

Berruti, F. M., Cedric, S., & Briens, L. (2013). Development and Applications of a Novel Intermittent Solids Feeder for Pyrolysis Reactors Graduate Program in Chemical and Biochemical Engineering. Retrieved from http://ir.lib.uwo.ca/etd

Bridgwater. (2007). Biomass Pyrolysis. *IEA Bioenergy: T34:2007:01*, 1–20. Retrieved from http://www.ieabioenergy.com/wp-content/uploads/2013/10/Task-34-Booklet.pdf

Bridgwater, A. V., Carson, P., & Coulson, M. (2007). A comparison of fast and slow

pyrolysis liquids from mallee. *International Journal of Global Energy Issues*, *27*(2), 204. https://doi.org/10.1504/IJGEI.2007.013655

Bridgwater, A. V, Meier, D., & Radlein, D. (1999). An overview of fast pyrolysis of biomass. Retrieved from https://ac.els-cdn.com/S0146638099001205/1-s2.0-S0146638099001205-main.pdf?_tid=c560041e-bfeb-11e7-b02f-00000aab0f6c&acdnat=1509640681_c30ef246c1a8baf455c37733c161230d

Bruun, S., Harmer, S. L., Bekiaris, G., Christel, W., Zuin, L., Hu, Y., … Lombi, E. (2017). The effect of different pyrolysis temperatures on the speciation and availability in soil of P in biochar produced from the solid fraction of manure. https://doi.org/10.1016/j.chemosphere.2016.11.058

Budai, A., Zimmerman, ; A R, Cowie, A. L., Webber, J. B. W., Singh, B. P., Glaser, ; B, … Lehmann, J. (2013). Biochar Carbon Stability Test Method: An assessment of methods to determine biochar carbon stability. International Biochar Initiative Biochar Carbon Stability Test Method: An assessment of methods to determine biochar carbon stability. Retrieved from http://www.biochar-international.org/sites/default/files/IBI_Report_Biochar_Stability_Test_Method_Final.pdf

Burhenne, L., Messmer, J., Aicher, T., & Laborie, M.-P. (2013). The effect of the biomass components lignin, cellulose and hemicellulose on TGA and fixed bed pyrolysis. *Journal of Analytical and Applied Pyrolysis*, *101*, 177–184. https://doi.org/10.1016/j.jaap.2013.01.012

City of London. (n.d.). City Wastewater Treatment. Retrieved November 23, 2017, from https://www.london.ca/residents/Sewers-Flooding/Sewage-Treatment/Pages/Wastewater-Treatment.aspx

City of London, E. & E. S. D. (2017). *Greenway Wastewater Treatment Centre 2016 Annual Report*. Retrieved from https://www.london.ca/residents/Sewers-Flooding/Sewage-Treatment/Documents/GRNWY16-AODA.pdf

City of Ottawa. (2017). Wastewater collection and treatment | City of Ottawa. Retrieved November 22, 2017, from https://ottawa.ca/en/residents/water-and-environment/wastewater-and-sewers/wastewater-collection-and-treatment#biosolids

Engineering, C. (2017). The Chemical Engineering Plant Cost Index - Chemical Engineering. Retrieved November 22, 2017, from http://www.chemengonline.com/pci-home

EPA. (1994). A Plain English Guide to the EPA Part 503 Biosolids Rule. Retrieved from https://www.epa.gov/sites/production/files/2015-05/documents/a_plain_english_guide_to_the_epa_part_503_biosolids_rule.pdf

EPA. (1996). METHOD 3540C. Retrieved from https://www.epa.gov/sites/production/files/2015-12/documents/3540c.pdf

European Commission. (2001). Disposal and recycling routes for sewage sludge Part 2 – Regulatory report. Retrieved from http://europa.eu.int/comm/environment/pubs/home.htm

Fagbohungbe, M. O., Herbert, B. M. J., Hurst, L., Ibeto, C. N., Li, H., Usmani, S. Q., & Semple, K. T. (2016). The challenges of anaerobic digestion and the role of biochar in optimizing anaerobic digestion. *Waste Management*. Retrieved from https://ac.els-cdn.com/S0956053X16306870/1-s2.0-S0956053X16306870-main.pdf?_tid=04dbe33a-c7dd-11e7-96bc-00000aacb362&acdnat=1510513954_4bfd3c103f92cdabdb008a8edd0a87b5

Faria, W. M., de Figueiredo, C. C., Coser, T. R., Vale, A. T., & Schneider, B. G. (2017). Is sewage sludge biochar capable of replacing inorganic fertilizers for corn production? Evidence from a two-year field experiment. *Archives of Agronomy and Soil Science*, 1–15. https://doi.org/10.1080/03650340.2017.1360488

Femi, I., Titiladunayo, Mcdonald, A. G., Olorunnisola, @bullet, & Fapetu, P. (2012). Effect of Temperature on Biochar Product Yield from Selected Lignocellulosic Biomass in a Pyrolysis Process. *Waste and Biomass Valorization*.

https://doi.org/10.1007/s12649-012-9118-6

Fuchs, W., & Drosg, B. (2009). Detailed monitoring of two biogas plants and mechanical solid–liquid separation of fermentation residues. *Journal of Biotechnology*, *142*(1), 56–63. https://doi.org/10.1016/J.JBIOTEC.2009.01.016

Generalix, E. (2014). Soxhlet Extractor. Retrieved December 21, 2017, from https://glossary.periodni.com/glossary.php?en=Soxhlet+extractor

Gusiatin, Z. M., Kurkowski, R., Brym, S., & Wiśniewski, D. (2016). Properties of biochars from conventional and alternative feedstocks and their suitability for metal immobilization in industrial soil. *Environmental Science and Pollution Research*. https://doi.org/10.1007/s11356-016-7335-4

Hossain, M. K., Strezov, V., Chan, K. Y., Ziolkowski, A., & Nelson, P. F. (2011). Influence of pyrolysis temperature on production and nutrient properties of wastewater sludge biochar. *Journal of Environmental Management*, *92*, 223–228. https://doi.org/10.1016/j.jenvman.2010.09.008

Huang, C.-Y., Tsai, W.-T., Chen, J.-W., Lin, Y.-Q., & Chang, Y.-M. (2017). Characterization of biochar prepared from biogas digestate. *Waste Management*. Retrieved from https://ac.els-cdn.com/S0956053X17302908/1-s2.0-S0956053X17302908-main.pdf?_tid=f7522e40-c7dc-11e7-9c01-00000aacb35f&acdnat=1510513931_a3091176d8ebe5f0dff54212f428f372

IBI. (2017a). About Us | International Biochar Initiative. Retrieved November 14, 2017, from http://www.biochar-international.org/about

IBI. (2017b). International Biochar Initiative | International Biochar Initiative. Retrieved November 21, 2017, from http://www.biochar-international.org/

Kankariya, D. M., Cedric Briens, S., & Supervisor Dominic Pjontek, J. (2016). Agglomerate Formation and Heat Transfer study in a Novel Mechanically Fluidized Reactor Graduate Program in Chemical and Biochemical Engineering. Retrieved from http://ir.lib.uwo.ca/etd

Khan, S., Chao, C., Waqas, M., Peter, H., Arp, H., & Zhu, Y.-G. (2013). Sewage Sludge Biochar Influence upon Rice (Oryza sativa L) Yield, Metal Bioaccumulation and Greenhouse Gas Emissions from Acidic Paddy Soil. *Environmental Science and Technology*. https://doi.org/10.1021/es400554x

Kizito, S., Luo, H., Wu, S., Ajmal, Z., Lv, T., & Dong, R. (2017). Phosphate recovery from liquid fraction of anaerobic digestate using four slow pyrolyzed biochars: Dynamics of adsorption, desorption and regeneration. https://doi.org/10.1016/j.jenvman.2017.06.057

Koga, Y., Oonuki, H., Amari, T., Endo, Y., Kakurate, K., & Ose, K. (2007). Biomass Solid Fuel Production from Sewage Sludge with Pyrolysis and Co-firing in Coal Power Plant. *Mitsubishi Heavy Industries, Ltd. Technical Review*, *44*(2). Retrieved from https://pdfs.semanticscholar.org/ac98/f43db3806cb5b2681ec6994097802e4eb9e9.pdf

Kong, Z. (2014). Effects of Pyrolysis Conditions and Biomass Properties on Leachability and Recyclability of Inorganic Nutrients in Biochars Produced from Mallee Biomass Pyrolysis. Retrieved from https://espace.curtin.edu.au/bitstream/handle/20.500.11937/1956/225820_Kong 2015 .pdf?sequence=2

Lee, J. M., Soo, J., Jung, L., & Kim, R. (1995). PYROLYSIS OF WASTE TIRES WITH PARTIAL OXIDATION IN A FLUIDIZED-BED REACTOR, *20*(10), 969–976. Retrieved from https://ac.els-cdn.com/036054429500049M/1-s2.0-036054429500049M-main.pdf?_tid=49c8eca8-c333-11e7-9838-00000aab0f6b&acdnat=1510001250_d036981ed8ddb386e4b502b2fb089cee

Lehmann, J., & Joseph, S. (2009). Biochar for Environmental Management: An Introduction. Retrieved from http://www.biochar-international.org/images/Biochar_book_Chapter_1.pdf

Li, D.-C., & Jiang, H. (2017). The thermochemical conversion of non-lignocellulosic

biomass to form biochar: A review on characterizations and mechanism elucidation. *Bioresource Technology*, *246*, 57–68. https://doi.org/10.1016/j.biortech.2017.07.029

Liu, X., Chang, F., Wang, C., Jin, Z., Wu, J., Zuo, J., & Wang, K. (2018). Pyrolysis and subsequent direct combustion of pyrolytic gases for sewage sludge treatment in China. https://doi.org/10.1016/j.applthermaleng.2017.08.091

Magdziarz, A., & Werle, S. (2014). Analysis of the combustion and pyrolysis of dried sewage sludge by TGA and MS. *Waste Management*, *34*, 174–179. https://doi.org/10.1016/j.wasman.2013.10.033

Marchetti, R., & Castelli, F. (2013). Biochar from Swine Solids and Digestate Influence Nutrient Dynamics and Carbon Dioxide Release in Soil. *Journal of Environment Quality*, *42*(3), 893. https://doi.org/10.2134/jeq2012.0352

Marshall, A. (2013). Commercial Application of Pyrolysis Technology in Agriculture. Retrieved from https://ofa.on.ca/uploads/userfiles/files/Pyrolysis Report Final.pdf

Méndez, A., Gómez, A., Paz-ferreiro, J., & Gascó, G. (2012). Chemosphere Effects of sewage sludge biochar on plant metal availability after application to a Mediterranean soil, *89*, 1354–1359. https://doi.org/10.1016/j.chemosphere.2012.05.092

Mesa-Pérez, J. M., Rocha, J. D., Barbosa-Cortez, L. A., Penedo-Medina, M., Luengo, C. A., & Cascarosa, E. (2013). Fast oxidative pyrolysis of sugar cane straw in a fluidized bed reactor. *Applied Thermal Engineering*, *56*, 167–175. https://doi.org/10.1016/j.applthermaleng.2013.03.017

Milhé, M., Van De Steene, L., Haube, M., Commandré, J.-M., Fassinou, W.-F., & Flamant, G. (2013). Autothermal and allothermal pyrolysis in a continuous fixed bed reactor. *Journal of Analytical and Applied Pyrolysis*, *103*, 102–111. https://doi.org/10.1016/j.jaap.2013.03.011

Nanda, S., Ajay Dalai, B. K., Franco Berruti, B., Janusz Kozinski, B. A., & Kozinski, J. A. (2016). Biochar as an Exceptional Bioresource for Energy, Agronomy, Carbon

Sequestration, Activated Carbon and Specialty Materials. *Waste and Biomass Valorization*, *7*, 201–235. https://doi.org/10.1007/s12649-015-9459-z

Oda, T. (2007). MAKING FUEL CHARCOAL FROM SEWAGE SLUDGE FOR THERMAL POWER GENERATION PLANT -FIRST IN JAPAN. Retrieved from http://www.gesui.metro.tokyo.jp/english/pdf/tp0701.pdf

Olsson, M., Kjällstrand, J., & Ran Petersson, G. (2003). Oxidative pyrolysis of integral softwood pellets. *Journal of Analytical and Applied Pyrolysis*, *67*, 135–141. Retrieved from www.elsevier.com/locate/jaap

Ontario, T. G. of. Nutrient Management Act (2002). Retrieved from http://www.compost.org/English/PDF/Nutrient_Management_Act.pdf

Peters, M. S., Timmerhaus, K. D., & West, R. E. (1991). *Plant Design and Economics for Chemical Engineers*. *Plant Design and Economics for Chemical Engineers*.

Peters, M., Timmerhaus, K., & West, R. (2002). Equipment Costs for Plant Design and Economics for Chemical Engineers - 5th Edition. Retrieved November 22, 2017, from http://www.mhhe.com/engcs/chemical/peters/data/

Shabangu, S., Woolf, D., Fisher, E. M., Angenent, L. T., & Lehmann, J. (2014). Techno-economic assessment of biomass slow pyrolysis into different biochar and methanol concepts. *FUEL*, *117*, 742–748. https://doi.org/10.1016/j.fuel.2013.08.053

Shariff, A., Aziz, N. S. M., Saleh, N. M., & Ruzali, N. S. I. (2016). The Effect of Feedstock Type and Slow Pyrolysis Temperature on Biochar Yield from Coconut Wastes. *7HE 1NFLUENCE 0F 7EMPERA7URE AND HEA71N6 RA7E 0N 7HE 5L0W PYR0LY515 0F 810MA55* , *10*(12). Retrieved from http://waset.org/publications/10005789/the-effect-of-feedstock-type-and-slow-pyrolysis-temperature-on-biochar-yield-from-coconut-wastes

Shen, Y., Forrester, S., Koval, J., & Urung-Demirtas, M. (2017). Yearlong semi-continuous operation of thermophilic two-stage anaerobic digesters amended with biochar for enhanced biomethane production. *Journal of Cleaner Production*.

Retrieved from https://ac.els-cdn.com/S095965261731079X/1-s2.0-S095965261731079X-main.pdf?_tid=be2584be-c7dc-11e7-96c6-00000aacb35e&acdnat=1510513835_82d5e7eb9a1b711602f7067610cbed85

Sousa, A. A. T. C., & C.C", F. (2015). Sewage sludge biochar: effects on soil fertility and growth of radish. *Biological Agriculture & Horticulture*, *32*(2), 127–138. Retrieved from http://www.tandfonline.com/doi/pdf/10.1080/01448765.2015.1093545?needAccess=true

Spokas, K. A. (2010). Review of the stability of biochar in soils: predictability of O:C molar ratios. *Carbon Management*. Retrieved from https://pubag.nal.usda.gov/pubag/downloadPDF.xhtml?id=47731&content=PDF

Su, Y., Luo, Y., Wu, W., Zhang, Y., & Zhao, S. (2012). Characteristics of pine wood oxidative pyrolysis: Degradation behavior, carbon oxide production and heat properties. *Journal of Analytical and Applied Pyrolysis*, *98*, 137–143. https://doi.org/10.1016/j.jaap.2012.07.005

Tan, C., Yaxin, Z., Hongtao, W., Wenjing, L., Zeyu, Z., Yuancheng, Z., & Lulu, R. (2014). Influence of pyrolysis temperature on characteristics and heavy metal adsorptive performance of biochar derived from municipal sewage sludge. *BIORESOURCE TECHNOLOGY*, *164*, 47–54. https://doi.org/10.1016/j.biortech.2014.04.048

Tumbalan-Gooty, A. (2014). *published Akhil thesis*.

Wellinger, A., Murphy, J., & Baxter, D. (2013). *The biogas handbook : science, production and applications*. Retrieved from https://books.google.ca/books?hl=en&lr=&id=NFxEAgAAQBAJ&oi=fnd&pg=PA267&dq=digestate+quality&ots=KD4jXwG5a2&sig=4nCKSuPEbCkUNJHmx5FXU-e0C7E#v=onepage&q=digestate quality&f=false

Williams, P., & Besler, S. (1996). The Influence of Temperature ans Heating Rate on the

Slow Pyrolysis of Biomass. *Renewable Energy*, *7*(3), 233–250. Retrieved from https://ac.els-cdn.com/0960148196000067/1-s2.0-0960148196000067-main.pdf?_tid=0280e888-cedb-11e7-b957-00000aacb35d&acdnat=1511282749_ea82e999a358fa7721dcb2b0947c70b8

Yuan, H., Lu, T., Dandan, @bullet, @bullet, Z., Huang, H., Kobayashi, @bullet, … Chen, Y. (2013). Influence of temperature on product distribution and biochar properties by municipal sludge pyrolysis. https://doi.org/10.1007/s10163-013-0126-9

Zhang, Z., Yani, S., Zhu, M., Li, J., & Zhang, D. (2013). Effect of Temperature and Heating Rate in Pyrolysis on the Yield, Structure and Oxidation Reactivity of Pine Sawdust Biochar. Retrieved from http://www.conference.net.au/chemeca2013/papers/30430.pdf

6 APPENDICES

6.1 Appendix A: Economic Analysis Assumptions

The following is a summary of the assumptions made to complete the economic analysis shown in Chapter 3.2.5.

Table 6.1: Initial Equipment Capacities and Purchase Equipment Costs

Equipment (Capacity Unit)	Initial Quote Capcity	Quoted Cost
Belt Dryer (ton h20 per day)	26.5	$250,000.00
Char Storage (total volume m3)	5400	$306,000.00
Pyrolysis Gas Burner (heat Duty kW)	4900	$423,000.00
Rotary Kiln Pyrolyzer (throughput dry tons per day)	24	$965,000.00
Scrubber (Gas throughput (kg per hr))	20000	$120,000.00

Table 6.2: Assumptions for Direct Capital Costs

Expense	Assumptions
Installation	39% of Total Purchased Equipment Costs
Piping	31% of Total Purchased Equipment Costs
Instrumentation and Control	26% of Total Purchased Equipment Costs
Electrical Installation	10% of Total Purchased Equipment Costs
Building and Services	29% of Total Purchased Equipment Costs
Land and Site Development	12% of Total Purchased Equipment Costs
Utilities and service facilities	55% of Total Purchased Equipment Costs

Table 6.3: Assumptions for Indirect Capital Costs

Expense	Assumptions
Engineering and Supervision	30% of Total Purchased Equipment Costs
Construction Expenses	35% of Total Purchased Equipment Costs
Contractor's fees	20% of Total Purchased Equipment Costs
Contingencies	30% of Total Purchased Equipment Costs

Table 6.4: Assumptions for Total Capital Investment

Expense	Assumptions
Total Capital Costs	Fixed + direct + indirect capital costs
Working Capital	5% of Total Capital Costs
Total Capital Investment	Total Capital + Working Capital

Table 6.5: Assumptions for Direct Production Costs

Expense	Assumptions
Labour Costs	2 operators working 3 shift per day at $50K per year
Utilities (electricity)	$0.09 per kWh
Utilities (naturla Gas)	$0.15/m^3
Maintenance and repair	6% of Total Purchased Equipment Costs
Operating Supplies	15% of Maintenance Costs
Laboratory Expenses	15% of labour costs

Table 6.6: Assumptions for Indirect Production Costs

Expense	Assumptions
Overhead (Benefits, EI)	40% of labour costs
Insurance and Property Tax	2% of fixed capital investment

Table 6.7: Assumptions for Annual General Expenses

Expense	Assumptions
Administrative Costs	25% of overhead
Research and Development	5% of annual total expenses
Distribution and Sales	10% of annual total expenses

Curriculum Vitae

Name: Devon Barry

Post-secondary Education and Degrees: The University of Western Ontario
London, Ontario, Canada
2011-2015 B.E.Sc. in Chemical Engineering

Honours and Awards: Western Graduate Scholarship
2015-2017,

Related Work Experience Graduate Research Assistant
Institute for Chemicals and Fuels from Alternative Resources
(ICFAR) The University of Western Ontario
2015-2017